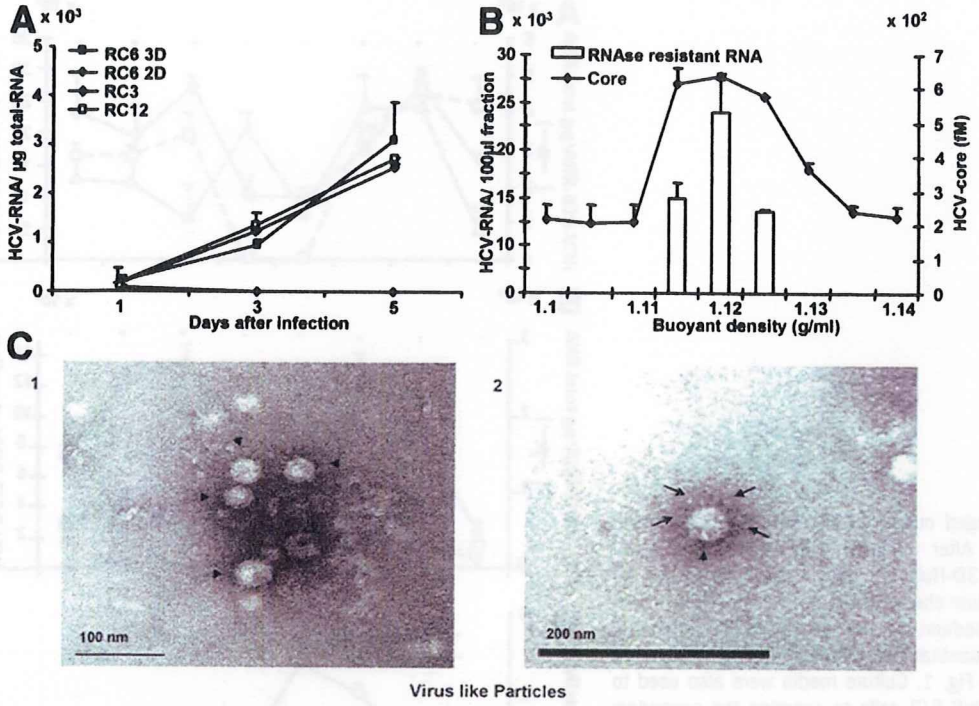

Fig. 2. Production of infectious virus-like particles from 3D-HuS-E/2 cells infected with different HCV strains. (A) The culture medium of 3D-HuS-E/2 cells infected with HCV-RC3 or HCV-RC6 was collected from days 5 to 7 p.i. and for HCV-RC12 from days 23 to 25 p.i. The culture medium of 2D-HuS-E/2 cells infected with HCV-RC6 was also collected from days 5 to 7 p.i., and used to treat naïve 3D-HuS-E/2 cells. The quantity of HCV genomic RNA in 1 μg of total cellular RNA was determined as in Fig. 1. (B) The concentrated culture medium of 3D-HuS-E/2 cells infected with HCV-RC3 was collected from days 5 to 7 p.i., and fractionated by ultracentrifugation with a 20%-50% sucrose density gradient. HCV-core protein and the RNase A-resistant HCV-RNA in the different fractions were quantitatively analyzed using an HCV-core ELISA kit and real-time RT-PCR, respectively. Data represent the mean ± SD of three independent experiments. (C) Photomicrograph showing negatively stained virus-like particles from the culture medium of HCV-RC3-infected 3D-HuS-E/2 cells (arrowheads, panels 1 and 2). The arrows indicate the spike-like structures found on the surface of the virus-like particles (panel 2).

RC3, RC6, and RC12 were used for infection, it was undetectable when RC2, P17, P27, and P33 sera were used, similar to 2D-HuS-E/2 cells infected with HCV-RC6 (Fig. 1C).

Production of Infectious Particles from 3D-HuS-E/2 Cells Infected with bbHCV. The culture media from 2D or 3D-HuS/E2 cells infected with RC6 serum (Fig. 1A) were collected from days 5 to 7 postinfection (p.i.), concentrated, and inoculated into naïve 3D-HuS-E/2 cell culture media. HCV-RNA's proliferation in the infected cells was only detected when using the culture medium from 3D-HuS-E/2 cells and not 2D-HuS-E/2 cells (Fig. 2A). Media collected from HCV-RC3 at days 5 to 7 and from HCV-RC12 from days 23 to 25 p.i. were also able to infect naïve cells (Fig. 2A). These data suggested the production and secretion of infectious virus-like particles. To investigate this further, biophysical analysis was performed. The culture medium of HCV-RC3 infected 3D-HuS-E/2 cells at day 7 p.i. was fractionated using a sucrose density gradient after RNase A treatment. HCV core was detected in the 1.11 to 1.14 g/mL fractions; similarly, the nuclease-resistant HCV RNA peaked in the 1.12 g/mL fraction (Fig. 2B). Furthermore, only the 1.12 g/mL fraction was able to infect naïve cells as examined above (data not shown). This fraction was pelleted by ultracentrifugation and examined by electron microscopy with negative staining. We observed 33-nm to 45-nm diameter spherical particles (Fig. 2C, panel 1) with spike-like structures from 7-9 nm in length on the surface (Fig. 2C, panel 2), consistent with HCV morphology reported previously in HCV patients.[18] These were detected in the sample collected from HCV-RC3-treated but not mock-treated 3D-HuS-E/2 cells. These data suggest that production of infectious virus-like particles occurs in 3D-HuS-E/2 cells infected with some bbHCV strains. It is therefore likely that 3D-HuS-E/2 cells can be used to reproduce nearly all steps in the HCV life cycle.

Prolonged Culture of HCV-Infected Cells in the 3D Hollow Fiber System. For HCV-RC6-infected cells (Fig. 3A), the amount of HCV-RNA in the cells fluctuated during the 30-day culture period. The levels of both HCV-RNA and HCV-core in the medium showed a similar pattern of fluctuations that peaked on days 5 and 20 p.i. Unlike RC6, the pattern of HCV-RNA levels in the medium of RC12-infected cells showed a negative

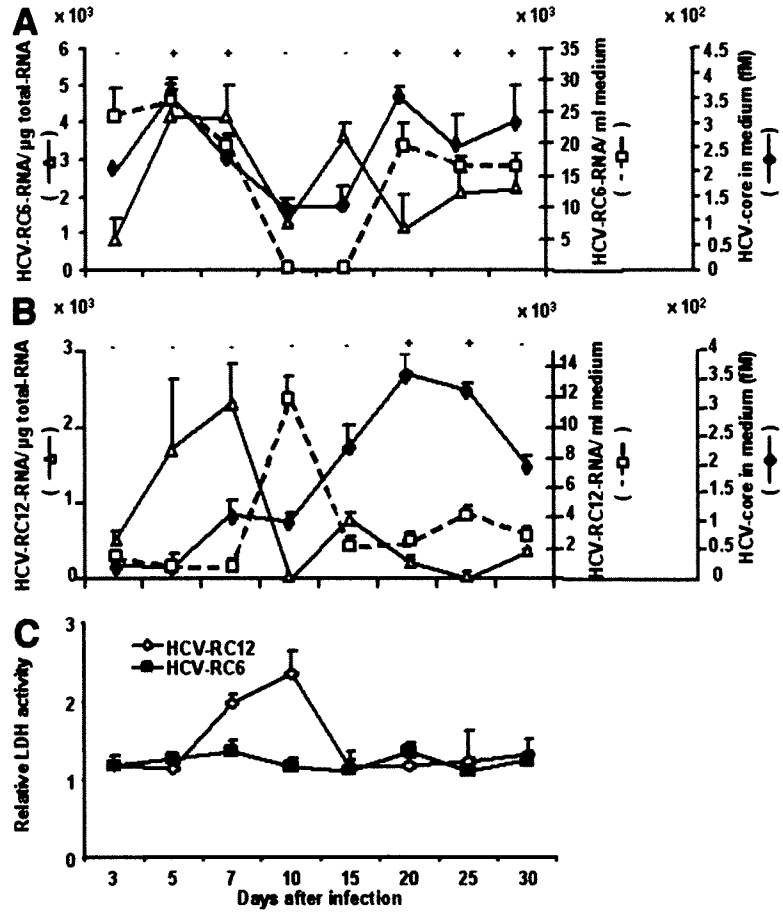

Fig. 3. Prolonged culture of HCV-infected cells in the 3D/HF system. After infection with HCV-RC6 (A) and HCV-RC12 (B), 3D-HuS-E/2 cells were cultured for 30 days with a medium change every 2 days. The HCV-RNA in the cells and medium as well as the HCV-core in the medium were quantitatively analyzed at the designated timepoints as in Fig. 1. Culture media were also used to treat naïve 3D-HuS-E/2 cells to examine the secondary infection as in Fig. 2. (+) and (−) indicate detection or no detection of secondary infection. (C) Culture media of HCV-RC6 and HCV-RC12 infected cells collected at each timepoint were used for the detection of LDH levels released from dead cells. LDH levels were normalized to uninfected cells cultured for the same time. Data represent the mean ± SD of three independent experiments.

correlation with that detected in the cells. This was clearly seen on day 10 p.i., when a sharp increase and decrease of HCV-RNA in the medium and the cells, respectively, was observed (Fig. 3B). Similarly, the amount of HCV-core detected in the medium throughout the culture was not correlated with RNA levels in the medium. Instead, core levels were very low in the first 10 days, at which time levels increased, reaching a peak on day 20 p.i. (Fig. 3B). Culture media from cells infected with HCV-RC6 from days 5 to 7 and 20 to 30 p.i. (Fig. 3A) and that from HCV-RC12 from days 20 to 25 p.i. showed passage of infectivity (Fig. 3B). All culture media showing infectivity appeared to have a high amount of HCV-core protein.

Clonal Changes in HCV During Prolonged Culture. In order to perform a populational analysis to understand the fluctuating pattern seen during HCV proliferation, two sera with limited HCV variants, HCV-RC6 (two major strains) and -RC12 (single major strain) from immunosuppressed liver transplantation patients with recurrent HCV were used in the previous prolonged infection experiment. The variants' composition was analyzed by single-strand confirmation polymorphism analysis for HCV-HVR1 (Supporting Fig. 4). RC6 serum (Fig. 4A) showed two different major sequences, HCV-RC6-1 and -2 strains, which constituted 60% and 40%, respectively, and shared 85% homology. In cells infected with HCV-RC6 the nucleotide sequence of HVR1 on day 5 showed 97% homology to HCV-RC6-1, and on day 20 p.i. it showed 97% homology to HCV-RC6-2. These data suggest selection of the dominant HCV strain in the cells over time. For RC12 (Fig. 4B), the nucleotide sequence on day 5 p.i. had only one nucleotide difference from that of the HCV from the original serum. The sequence from day 20 p.i. was four nucleotides different from that from the serum, and five different from the cells on day 5 p.i. These data indicated that each peak of HCV-RNA that appeared in the cells infected with RC12 serum included primarily a single HCV strain with a slightly different genomic sequence. This suggests that the periodic appearance of HCV-RNA peaks in the cells infected with a particular HCV strain is a result of selection and/or mutation of HCV strains during the prolonged culture period.

Cellular Response Induced by bbHCV Infection. At day 10 p.i., HCV-RNA levels in the culture medium rose and RNA levels in 3D-HuS-E/2 cells infected with HCV-RC12 dropped (Figs. 1B, 3B). To determine if this was caused by a cytotoxic effect of HCV infection, LDH levels were measured in the culture medium of HCV-RC6- and

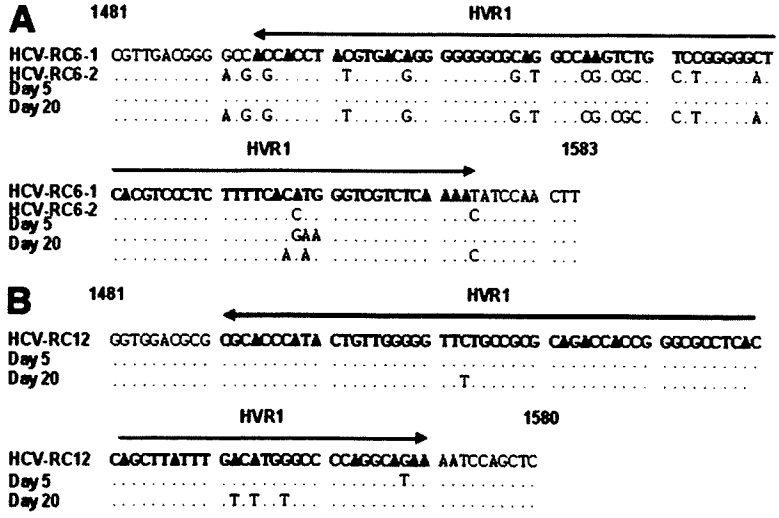

Fig. 4. Comparison of HCV-HVR1 sequences in the serum used for infection and the HCV replicating in the cells on days 5 and 20 after infection of HCV-RC6 (A) or HCV-RC12 (B). Nucleotide numbering was based on HCV-J1 sequence (GenBank Access. No. D10749). Three additional nucleotides were found at the 5′-terminal end of the E2 regions of all RC6 sequences. The major sequence present in the serum used for infection is shown in the upper row in each panel. Dots represent the identical nucleotides.

HCV-RC12-infected 3D-HuS-E/2 cells. LDH activity showed a strong correlation with HCV-RNA levels in the medium on day 10 p.i. in HCV-R12-infected cells (Fig. 3B), suggesting a cytotoxic effect of HCV-RC12 that was not observed in the case of HCV-RC6 (Fig. 3A,C). To determine if this HCV infection-mediated cytotoxicity is due to apoptosis, as with other viruses belonging to the Flaviviridae family,[19] the involvement of caspase was examined using the caspase inhibitor z-VAD-fmk. A significant dose-dependent reduction in HCV-RNA levels in the medium and LDH activity (Fig. 5A,B) was found, whereas no significant effect was observed on the viability of noninfected cells (Fig. 5B) or intracellular HCV-RNA levels (Fig. 5A). This suggested that the cytotoxic effect of HCV infection is mediated by apoptosis. It is noteworthy that HCV-induced cytopathicity was also found when HCV-P17 and HCV-P33 samples were used for infection (both are HCV-2a genotype) and was not reproduced in any of the HCV-1b genotype samples used in this work (Fig. 5C).

After infection with HCV-RC6, no cytotoxicity was detected that might have inhibited HCV-RC6-1 proliferation in the cells. However, HCV-RC6-2 RNA replaced HCV-RC6-1 RNA during prolonged culture. To assess a

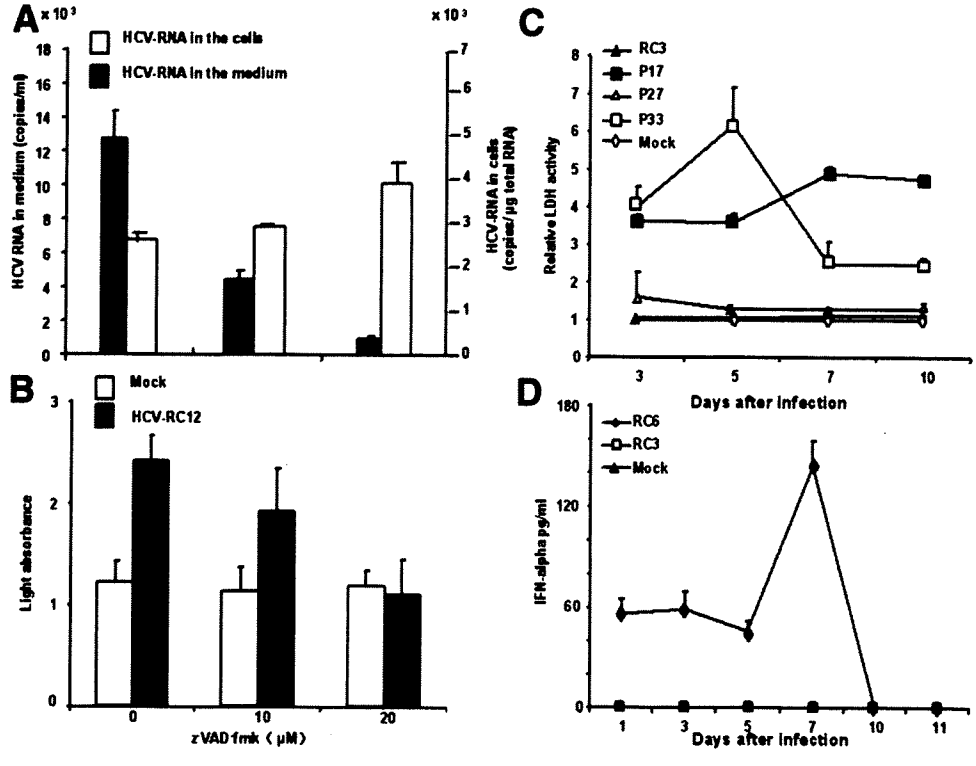

Fig. 5. Cellular response of 3D-HuS-E/2 cells infected with bbHCV. 3D-HuS-E/2 cells infected with HCV-RC12 and mock-treated cells were cultured for 10 days in the presence of z-VAD-fmk (0, 10, and 20 μM). (A) HCV-RNA in the cells and medium on day 10 was measured as in Fig. 1. (B) LDH levels in the medium on day 10 after infection with HCV-RC12 was measured as in Fig. 3. (C) Culture media of HCV-RC3, HCV-P17, HCV-P27, HCV-P33, and mock-infected cells collected at designated points were used for the detection of LDH levels. (D) IFN-α levels in the culture media of HCV-RC6, HCV-RC3, and mock-infected cells collected at each designated timepoint were measured by ELISA. Data represent the mean $\pm$ SD of three independent experiments.

possible role of the innate-immune response in this phenomenon, the production of IFN-α in the medium was measured during the first 11 days p.i. IFN-α production was detected as early as day 1 p.i., reached a peak at day 7 p.i., and was then rapidly lost (Fig. 5D). These data suggest that HCV-RC6-1 infection induced the innate-immune response of the cells, possibly leading to suppression of its proliferation. In contrast to HCV-RC6-1, HCV-RC3 did not show any stimulation of IFN-α production upon infection in the first 10 days, showing a possible strain-dependent evasion from the host defense within the same genotype.

Discussion

In this study we report the development of a novel system that reproduces bbHCV infection, proliferation, and production of infectious virus. The most recent models used in the study of the life cycle of HCV infection are based on subclones of HuH-7 cells infected with JFH1 recombinant virus or its derivatives.[4] HuH-7 cells and its subclones, however, do not support the entire life cycle of the bbHCVs present in patients' blood.[5] Moreover, HCV has considerable diversity and variability. It is generally classified into six major genotypes and more than 100 subtypes.[20] This huge pool of natural HCV variants causes a wide variety of diseases, including chronic hepatitis, cirrhosis, and hepatocellular carcinoma.[21] JFH1, however, is a single isolate of HCV genotype 2a that was originally derived from a patient with rare fulminant hepatitis.[4] We suggest that our newly established system has an important advantage because it supports the entire life cycle of a variety of HCV strains and genotypes.

Due to the lack of some *in vivo* factors, including host immune response, *in vitro* systems may not completely reproduce the *in vivo* situation. However, *in vitro* experimental systems seem to be important to simplify particular events from the complex situation *in vivo*. From that standpoint, our cell culture system is likely reproducing the early event of HCV infection in the absence of host-immune responses and supporting whole life cycle of the blood-borne HCV. Several *in vitro* hepatocyte culture systems have been reported to be useful for studying the infection and replication of bbHCV.[5-8,22] Only the radial-flow bioreactor (RFB) 3D culture system demonstrated production of infectious viruses.[22] In our studies we observed not only the enhancement of HCV replication, but also the production of infectious HCV particles in the medium using the 3D/HF system. These data suggest that some structure of the cell mass formed by the 3D culture system, most likely the polar character, is essential for the life cycle of bbHCV. The RFB system is composed of a dedicated device containing 1×10^9 FLC4 cells with a culture area of 2.7 m^2.[22] It can only be used to study HCV particle production in the medium and not the cellular events that accompany the HCV life cycle. In contrast, because cells grown in our 3D/HF system are cultured in 12-well plates at a density of 3×10^5/fiber, it is much simpler to study both viral and cellular events.

The production of infectious particles was not detected with infection by different HCV strains, despite detecting equivalent levels of HCV-RNA in the cells (Fig. 1B,C). Delayed production of infectious particles was also observed in cells infected with HCV-RC12 after prolonged culture. A similar delay was also observed in the RFB system.[22] Considering the relative stability of HuS-E/2 cells[5] and the relatively high frequency of the change in HCV population in the cells,[16] it is likely that mutation of the HCV genome and/or selection of clones during prolonged culture improved the productivity of infectious particles. A marked improvement of infectious particle production by substitution of the structural proteins of the genome was also reported in the recombinant HCV production system.[23] The lack of production of infectious particles soon after infection may serve to avoid an early strong response from the host immune system, and demonstrates a novel mechanism of latent infection by HCV. Although they may not be associated with plasma components as those present *in vivo*, HCV virus-like particles produced by this system showed a close resemblance to those isolated from infected HCV patients because they showed the same size[18] and were within the fraction range.[24] They may help in the study of viral and cellular factors required for particle production and the possible receptors utilized for infection with different HCV strains.

Fluctuation in HCV proliferation was observed during the prolonged culture of 3D-HuS-E/2 cells infected with bbHCV (Fig. 3A,B), consistent with previous reports in other culture systems.[6,22] This fluctuation was associated with a change in viral quasispecies, suggesting that an HCV strain having a growth advantage proliferates selectively and dominantly in these culture conditions. Because the progressive emergence of each dominant strain was only temporary, it is highly likely that the infection and proliferation of such an HCV strain is suppressed by cellular mechanism(s). Our results suggest that there are actually two cellular mechanisms functioning to do this. The first is the involvement of the innate immune system, as evidenced by the secretion of IFN-α during the first week of infection (Fig. 5D). This is the first report of secretion of IFN-α from cultured cells infected with bbHCV. Although recent reports suggest that stimulation of the IFN pathway by HCV infection could be impaired by HCV NS3-4a proteinase-mediated cleavage of IPS-

1,[25] our results suggest that not all bbHCVs possess a host cell suppressive function. The second mechanism is HCV-induced cell death (Fig. 3C). Almost all the studies reporting HCV-induced apoptosis used hepatocellular carcinoma cell lines.[26,27] Because it has been established that the inability to undergo apoptosis is essential for the development of cancer,[28-30] our use of immortalized, noncancerous HuS-E/2 hepatocytes may make it possible to reproduce the physiological response of the cells to bbHCV infection more closely. Although HCV-induced apoptosis was not found when HCV-1b was used for infection, it was found in all cases where HCV-2a was used, suggesting a higher cytopathic tendency of the HCV-2a genotype. HCV proliferation was continuously found even after the suppression of the first peak of RNA production during prolonged culture. How HCV survives under those conditions is still unknown. Further studies to clarify the molecular mechanisms involving the HCV-cell interaction can be done using this novel 3D culture system that reproduces the infection of a variety of bbHCVs.

In conclusion, we have established a new *in vitro* culture system that can support the entire life cycle of a variety of HCV isolates and genotypes. Although this *in vitro* model system may not completely reproduce the *in vivo* situation, we believe it is the first *in vitro* system showing HCV strain-dependent virus/cell interaction including induction of cellular apoptosis and/or evasion from cellular innate immune response, which may make it a good tool for analysis of virus/host interaction together with the development of new anti-HCV strategies for the different bbHCV strains.

Acknowledgment: We thank T. Yamaguchi for providing hollow fibers and culture medium.

References

1. Wasley A, Alter MJ. Epidemiology of hepatitis C: geographic differences and temporal trends. Semin Liver Dis 2000;20:1-16.
2. Younossi Z, Kallman J, Kincaid J. The effects of HCV infection and management on health-related quality of life. HEPATOLOGY 2007;45:806-816.
3. Fried MW, Shiffman ML, Reddy KR, Smith C, Marinos G, Goncales FL Jr, et al. Peginterferon alfa-2a plus ribavirin for chronic hepatitis C virus infection. N Engl J Med 2002;347:975-982.
4. Wakita T, Pietschmann T, Kato T, Date T, Miyamoto M, Zhao Z, et al. Production of infectious hepatitis C virus in tissue culture from a cloned viral genome. Nat Med 2005;11:791-796.
5. Aly HH, Watashi K, Hijikata M, Kaneko H, Takada Y, Egawa H, et al. Serum-derived hepatitis C virus infectivity in interferon regulatory factor-7-suppressed human primary hepatocytes. J Hepatol 2007;46:26-36.
6. Ikeda M, Sugiyama K, Mizutani T, Tanaka T, Tanaka K, Sekihara H, et al. Human hepatocyte clonal cell lines that support persistent replication of hepatitis C virus. Virus Res 1998;56:157-167.
7. Chong TW, Smith RL, Hughes MG, Camden J, Rudy CK, Evans HL, et al. Primary human hepatocytes in spheroid formation to study hepatitis C infection. J Surg Res 2006;130:52-57.
8. Molina S, Castet V, Pichard-Garcia L, Wychowski C, Meurs E, Pascussi JM, et al. Serum-derived hepatitis C virus infection of primary human hepatocytes is tetraspanin CD81 dependent. J Virol 2008;82:569-574.
9. El-Farrash MA, Aly HH, Watashi K, Hijikata M, Egawa H, Shimotohno K. In vitro infection of immortalized primary hepatocytes by HCV genotype 4a and inhibition of virus replication by cyclosporin. Microbiol Immunol 2007;51:127-133.
10. Mizumoto H, Ishihara K, Nakazawa K, Ijima H, Funatsu K, Kajiwara T. A new culture technique for hepatocyte organoid formation and long-term maintenance of liver-specific functions. Tissue Eng Part C Methods 2008; 14:167-175.
11. Funatsu K, Ijima H, Nakazawa K, Yamashita Y, Shimada M, Sugimachi K. Hybrid artificial liver using hepatocyte organoid culture. Artif Organs 2001;25:194-200.
12. Mizumoto H, Aoki K, Nakazawa K, Ijima H, Funatsu K, Kajiwara T. Hepatic differentiation of embryonic stem cells in HF/organoid culture. Transplant Proc 2008;40:611-613.
13. Andrei G. Three-dimensional culture models for human viral diseases and antiviral drug development. Antiviral Res 2006;71:96-107.
14. Hijikata M, Kato N, Ootsuyama Y, Nakagawa M, Ohkoshi S, Shimotohno K. Hypervariable regions in the putative glycoprotein of hepatitis C virus. Biochem Biophys Res Commun 1991;175:220-228.
15. Boulestin A, Sandres-Saune K, Payen JL, Alric L, Dubois M, Pasquier C, et al. Genetic heterogeneity of the envelope 2 gene and eradication of hepatitis C virus after a second course of interferon-alpha. J Med Virol 2002; 68:221-228.
16. Murakami K, Inoue Y, Hmwe SS, Omata K, Hongo T, Ishii K, et al. Dynamic behavior of hepatitis C virus quasispecies in a long-term culture of the three-dimensional radial-flow bioreactor system. J Virol Methods 2008;148:174-181.
17. Meuleman P, Hesselgesser J, Paulson M, Vanwolleghem T, Desombere I, Reiser H, et al. Anti-CD81 antibodies can prevent a hepatitis C virus infection in vivo. HEPATOLOGY 2008;48:1761-1768.
18. Kaito M, Watanabe S, Tsukiyama-Kohara K, Yamaguchi K, Kobayashi Y, Konishi M, et al. Hepatitis C virus particle detected by immunoelectron microscopic study. J Gen Virol 1994;75:1755-1760.
19. Roulston A, Marcellus RC, Branton PE. Viruses and apoptosis. Annu Rev Microbiol 1999;53:577-628.
20. Forns X, Bukh J. The molecular biology of hepatitis C virus. Genotypes and quasispecies. Clin Liver Dis 1999;3:693-716, vii.
21. Dickson RC. Clinical manifestations of hepatitis C. Clin Liver Dis 1997; 1:569-585.
22. Aizaki H, Nagamori S, Matsuda M, Kawakami H, Hashimoto O, Ishiko H, et al. Production and release of infectious hepatitis C virus from human liver cell cultures in the three-dimensional radial-flow bioreactor. Virology 2003;314:16-25.
23. Mateu G, Donis RO, Wakita T, Bukh J, Grakoui A. Intragenotypic JFH1 based recombinant hepatitis C virus produces high levels of infectious particles but causes increased cell death. Virology 2008;376:397-407.
24. Li X, Jeffers LJ, Shao L, Reddy KR, de Medina M, Scheffel J, et al. Identification of hepatitis C virus by immunoelectron microscopy. J Viral Hepat 1995;2:227-234.
25. Gale M Jr, Foy EM. Evasion of intracellular host defence by hepatitis C virus. Nature 2005;436:939-945.
26. Fischer R, Baumert T, Blum HE. Hepatitis C virus infection and apoptosis. World J Gastroenterol 2007;13:4865-4872.
27. Aoki H, Hayashi J, Moriyama M, Arakawa Y, Hino O. Hepatitis C virus core protein interacts with 14-3-3 protein and activates the kinase Raf-1. J Virol 2000;74:1736-1741.
28. Ladu S, Calvisi DF, Conner EA, Farina M, Factor VM, Thorgeirsson SS. E2F1 inhibits c-Myc-driven apoptosis via PIK3CA/Akt/mTOR and COX-2 in a mouse model of human liver cancer. Gastroenterology 2008; 135:1322-1332.
29. Lowe SW, Lin AW. Apoptosis in cancer. Carcinogenesis 2000;21:485-495.
30. Schulze-Bergkamen H, Krammer PH. Apoptosis in cancer—implications for therapy. Semin Oncol 2004;31:90-119.

Biochemical and Biophysical Research Communications 379 (2009) 330–334

Contents lists available at ScienceDirect

Biochemical and Biophysical Research Communications

journal homepage: www.elsevier.com/locate/ybbrc

3D cultured immortalized human hepatocytes useful to develop drugs for blood-borne HCV

Hussein Hassan Aly [a], Kunitada Shimotohno [b], Makoto Hijikata [a,c,*]

[a] Laboratory of Human Tumor Viruses, The Institute for Virus Research, Kyoto University, Department of Viral Oncology, 53 Kawaharacho, Shogoin, Sakyoku, Kyoto 606-8507, Japan
[b] Center for Human Metabolomic Systems Biology, Keio University, 35 Shinano-machi, Shinjuku-ku, Tokyo 160-8582, Japan
[c] Laboratory of Viral Oncology, Graduate School of Biostudies, Kyoto University, Konoecho, Yoshida, Sakyoku, Kyoto 606-8501, Japan

ARTICLE INFO

Article history:
Received 5 December 2008
Available online 25 December 2008

Keywords:
Hepatitis C virus
Infection
Replication
3D culture
PPAR
Immortalized hepatocytes
Blood-borne HCV

ABSTRACT

Due to the high polymorphism of natural hepatitis C virus (HCV) variants, existing recombinant HCV replication models have failed to be effective in developing effective anti-HCV agents. In the current study, we describe an *in vitro* system that supports the infection and replication of natural HCV from patient blood using an immortalized primary human hepatocyte cell line cultured in a three-dimensional (3D) culture system. Comparison of the gene expression profile of cells cultured in the 3D system to those cultured in the existing 2D system demonstrated an up-regulation of several genes activated by peroxisome proliferator-activated receptor alpha (PPARα) signaling. Furthermore, using PPARα agonists and antagonists, we also analyzed the effect of PPARα signaling on the modulation of HCV replication using this system. The 3D *in vitro* system described in this study provides significant insight into the search for novel anti-HCV strategies that are specific to various strains of HCV.

Infection with Hepatitis C virus (HCV) is a serious health problem worldwide and leads to high rates of liver cirrhosis and hepatocellular carcinoma [1]. Given that the standard HCV therapy remains insufficient for the successful treatment of many patients [2], the development of more effective and less toxic anti-HCV agents is required. *In vitro* systems like the HCV replicon-bearing cells and the infectious particle-producing JFH1 system, has contributed to the discovery of new targets for anti-HCV therapy. However, these recombinant HCV genomes only proliferate in sublines of HuH-7 cells, which do not permit infection or proliferation of blood-borne HCV. Due to the high polymorphism of natural HCV, data from recombinant HCV systems could be evaluated by studying the therapeutic response of a variety of naturally occurring HCVs. However, the current systems available for such study remain insufficient due to the low infection and replication efficiency of the natural HCV strains.

More recently, production and secretion of infectious HCV particles has been reported in two independent three-dimensional (3D) cell culture systems, termed the radial-flow bioreactor (3D/RFB) and the thermoreversible gelatin polymer (3D/TGP) systems. These results were not observed in monolayer cultures [3], suggesting that hepatocytes cultured in 3D more closely resemble liver cells *in vivo* [4] and thus support HCV proliferation. In addition, analysis of gene expression levels in 3D cultured cells revealed that the newly established immortalized human hepatocyte (HuS-E/2 cells) gene profile was altered to more closely resemble that of human liver tissue when the cells were cultured in 3D/TGP [5].

In the current study, we cultured HuS-E/2 cells in 3D/TGP and demonstrated efficient proliferation of natural HCV. Furthermore, gene expression analysis of these cells demonstrated the activation of the peroxisome proliferators-activated receptor α (PPARα) signaling pathway, suggesting an important role for this pathway in the replication of natural HCV. Thus, the *in vitro* system described appears to be a useful tool for the study of HCV infection and proliferation as well as for the development of effective anti-viral agents against various natural HCVs.

Materials and methods

Cell culture. Immortalized human hepatocytes (HuS-E/2) and LucNeo#2 replicon cells [6] were cultured as previously described [5,7]. For the 3D-TGP culture system, 1×10^5 HuS-E/2 cells were cultured in 1 ml Mebiol gel (Mebiol Inc., Kanagawa, Japan)/well in 12-well plates. Five hundred microliters of fresh medium was overlaid on the solidified gel, and was changed every 2 days. Cell

* Corresponding author. Address: Laboratory of Human Tumor Viruses, The Institute for Virus, Kyoto University, Department of Viral Oncology, 53 Kawaharacho, Shogoin, Sakyoku, Kyoto 606-8507, Japan. Fax: +81 75 751 3998.
E-mail address: mhijikat@virus.kyoto-u.ac.jp (M. Hijikata).

0006-291X/$ - see front matter © 2008 Elsevier Inc. All rights reserved.
doi:10.1016/j.bbrc.2008.12.054

extraction from the gel was done at the designated time points according to the manufacturer's protocol.

RNA extraction, reverse transcriptase polymerase chain reaction (RT-PCR) and real-time RT-PCR (Q-PCR). At the designated time points, total cellular RNA was extracted and 1 μg of total RNA was used as a template for RT-PCR and for the quantitative detection of HCV-RNA using real-time RT-PCR (Q-PCR) as previously described [10].

HCV infection experiment. HCV infection experiments were carried out using sera from patients infected with HCV. Infection in 2D culture was undertaken as previously described [5]. For 3D/TGP cultured cells, the gel was solidified, and 50 μl HCV-containing patient serum with a titer of 1×10^6 HCV-RNA/ml was added to the culture and mixed. The culture was continued until the cells were extracted. Following extraction from 3D-TGP, cells were centrifuged and washed three times thoroughly with PBS. RNA was then extracted from the cells as described above. HCV infection into HuS-E/2 cells was also examined in the presence of anti-E2 mouse monoclonal antibody (917) as outlined previously [8].

Treatment of cells with PPARα signaling agonists and antagonists. Fenofibrate or MK886 (Sigma–Aldrich, USA) were added to the culture medium of HuS-E/2 (2D-HuS-E/2) cells from day 0 of HCV infection; or the culture medium of LucNeo#2 replicon harboring cells. The cells were then cultured to the designated time point.

Microarray analysis. Gene expression profiles of 3D/TGP cultured HuS-E/2 cells were obtained by microarray analysis (3D-Genes Human 25, Toray, Tokyo, Japan) and compared to those of cells cultured in 2D.

Results

3D/TGP cultures enhance HCV proliferation in HuS-E/2 cells

Infection and proliferation of the HCV genotype 1b (HCV-RC5) derived from the serum of patient RC5 in HuS-E/2 cells cultured in 3D/TGP (3D/TGP-HuS-E/2 cells) was investigated and compared with that of HuS-E/2 cells cultured in 2D (2D-Hus-E/2). As outlined in Fig. 1A, the HCV-RNA levels in the 3D/TGP-HuS-E/2 cells were significantly higher at all of the time points examined following infection than in the 2D-HuS/E2 cells, suggesting that the 3D/TGP system greatly enhances the proliferation of naturally occurring HCV in HuS-E/2 cells. Similar results were also obtained for sera from additional patients (data not shown). To examine whether the infection is viral envelope-receptor mediated, the infection experiments using serum treated with anti-HCV-E2 antibody (α-E2) or with anti-tubulin (negative control) was also performed. Pre-incubation of the serum with α-E2 significantly reduced the total amount of HCV-RNA in the cells upon infection (Fig. 1B). This result suggested that the infection of natural HCV into 3D/TGP-HuS-E/2 cells was HCV-E2-dependent.

Inhibition of natural HCV replication in HuS-E/2 cells by Interferon

In order to test the effects of anti-viral agents on natural HCV replication in 3D/TGP HuS-E/2 cells, 50–100 U/ml of IFNα was added to the medium overlaying the HCV-RC5 infected 3D/TGP-HuS-E/2 cells. The two treatment concentrations resulted in the inhibition of HCV-RNA replication in 3D-HuS-E/2 cells by

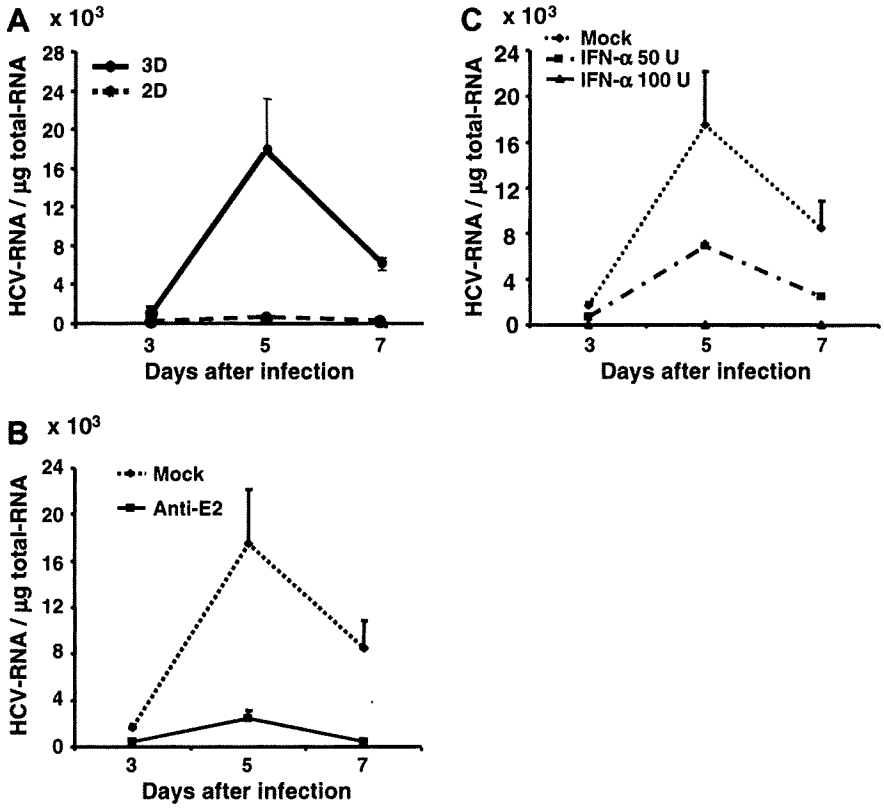

Fig. 1. HCV infection into 3D/TGP-HuS-E/2 cells. (A) 3D/TGP significantly enhanced HCV proliferation in HuS-E/2 cells. HCV patient serum was used to infect a similar number of HuS-E/2 cells cultured in 2D (hashed line) or 3D/TGP (solid line) culture for 24 h. Cells were then harvested and lysed at the indicated time points (3–7 days). The quantity of genomic HCV-RNA per 1 μg total RNA was determined by Q-PCR analysis. (B) Anti-E2 antibodies blocked HCV infection. HCV infection was performed as described in panel A in the presence of Anti-E2 specific or anti-tubulin (control) antibodies. (C) IFNα inhibits HCV replication in 3D/TGP-HuS-E/2 cells. HuS-E/2 cells were infected with HCV and fresh medium supplemented with or without (Mock), 50 U/ml, or 100 U/ml IFNα overlaid on the gel containing the cells and HCV proliferation measured as described above.

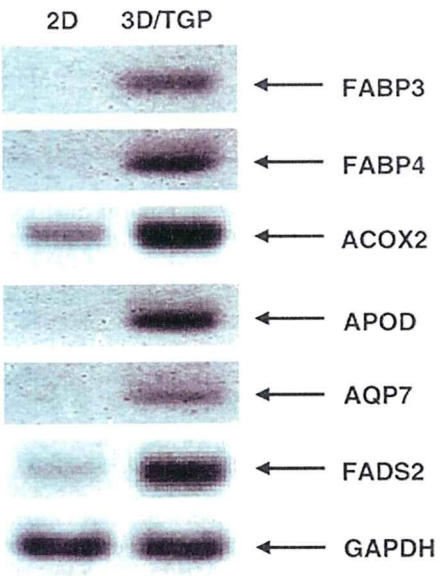

Fig. 2. RT-PCR analysis of the expression of genes identified by microarray. The PPARα regulated genes were increased in 3D/TGP-HuS-E/2 cells (3D-TGP) and their expression levels measured by RT-PCR. 2D represents RNA samples from 2D-HuS-E/2 cells. Twenty cycles of amplification were undertaken for the RT-PCR analysis. GAPDH expression served as an internal control. *Abbreviations:* FABP3, fatty acid binding proteins 3; FABP4, fatty acid binding proteins 4; ACOX2, acyl-coenzyme A oxidase 2; APOD, apolipoprotein D; AQP7, aquaporin 7; FADS2, fatty acid desaturase 2; GAPDH, glyceraldehyde 3-phosphate dehydrogenase.

approximately 50–60% and almost completely, respectively, when compared to the replication in cells receiving mock treatment (Fig. 1C). These results demonstrate that the IFNα treatment was effective on HCV derived from RC5 and that 3D/TGP-HuS-E/2 cells may be useful for the screening of anti-HCV drugs for the treatment of natural HCV.

Increased activation of the PPARα signaling pathway in 3D cultured HuS-E/2 cells

Given that 3D/TGP-HuS-E/2 cells demonstrated enhanced proliferation of natural HCV, the gene expression profiles of these cells was compared with that of cells cultured under normal 2D conditions using microarray analysis in order to identify the factors required for the enhanced proliferation. Among the 24,268 genes compared in this analysis, 212 genes demonstrated a greater than four folds index increase in expression in 3D/TGP than standard cultured cells. Cell signaling pathway analysis of these 212 genes showed that six genes, including fatty acid binding proteins 4 and 3 (FABP4 and 3), apolipoprotein D (APOD), aquaporin 7 (AQP7), acyl-coenzyme A oxidase 2 (ACOX2), and fatty acid desaturase 2 (FADS2), were targets of PPARα signaling [9–12]. The increased expression of these genes in the 3D/TGP-HuS-E/2 cells was further confirmed by RT-PCR analysis (Fig. 2). Given that PPARα is an essential factor for normal hepatocyte function [13], these results indicate that 3D/TGP culture enhances the hepatocyte-specific characteristics of HuS-E/2 cells.

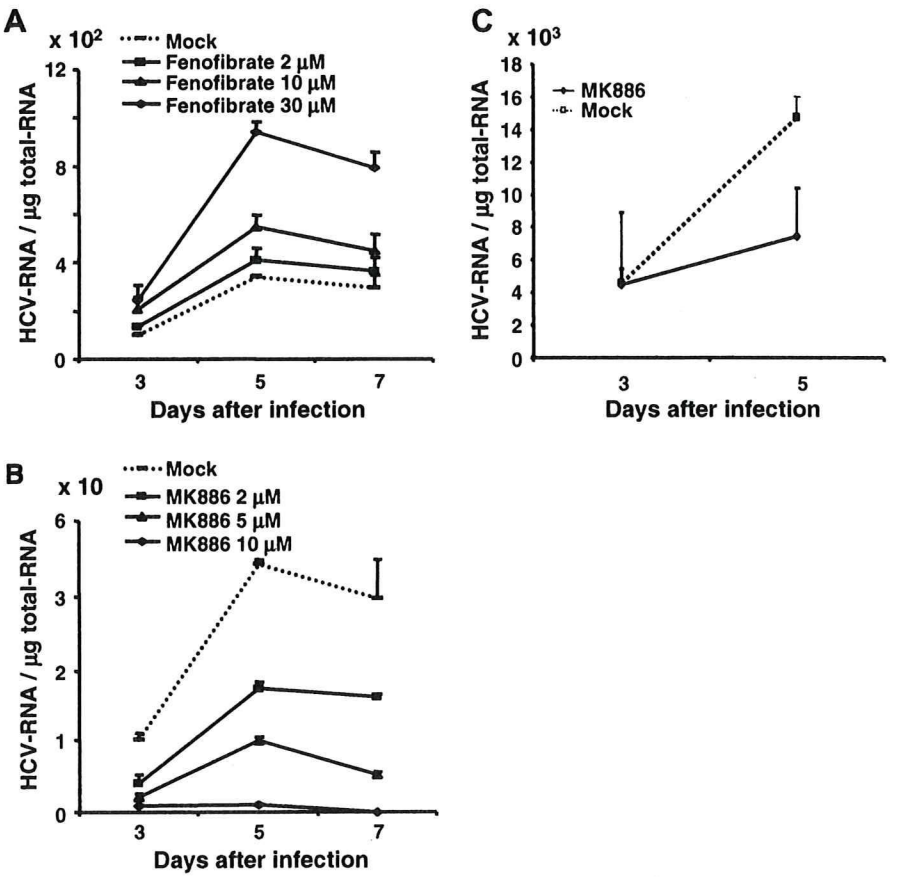

Fig. 3. The effects of PPARα agonists and antagonists on natural HCV proliferation. (A) HuS-E/2 cells were infected with HCV and fresh medium supplemented with or without (Mock) 2, 10, or 30 μM of fenofibrate overlaid on the cells. (B) Medium supplemented with or without (Mock), 2, 5, or 10 μM of MK886 was overlaid on 2D-HuS-E/2 cells infected with HCV. HCV proliferation following treatment was measured by Q-PCR. (C) Medium supplemented with or without (Mock), 10 μM of MK886 was overlaid on 3D/TGP-HuS-E/2 cells infected with HCV. HCV proliferation following treatment was measured by Q-PCR.

PPARα signaling affects HCV replication

We next examined the potential role of PPARα signaling on HCV proliferation by monitoring HCV replication in 2D-HuS-E/2 cells that had been infected with HCV-RC5 and subsequently treated with the PPARα agonist fenofibrate [14] or the PPARα antagonist MK886 [14] (Fig. 3B). As outlined in Fig. 3A, a dose-dependent increase in HCV replication was observed in fenofibrate-treated cells. In contrast, a dose-dependent decrease in HCV proliferation was observed in the presence of MK886. Similarly, treatment with MK886 reduced HCV proliferation in 3D/TGP-HuS-E/2 cells (Fig. 3C). The response of HCV proliferation in response to fenofibrate and MK886 treatment was also analyzed in LucNeo#2 cells that contained HCV replicon RNA (LNMH14) derived from the HCV-1b genome (Fig. 4A). Luciferase expression in these cells represented replication of the HCV replicon [6] and, as shown in Fig. 4A, luciferase activity in the cells treated with fenofibrate or MK886 also showed either enhancement or suppression of replicon proliferation, respectively. In addition, the increased HCV replication following fenofibrate treatment was completely abolished when treated with MK886 simultaneously. As MK886 is known to induce apoptosis when administered in high doses [15], the cell viability was examined using the XTT assay. There were no significant effects on cell viability after treatment with fenofibrate. Although MK886 resulted in a minor reduction in XTT values when high doses (10–15 μM) were administered, this reduction was not statistically significant when compared to its effect on HCV replication (Fig. 4B). This result suggests that PPARα signaling is required for HCV replication and that suppression of PPARα signaling has an anti-HCV effect.

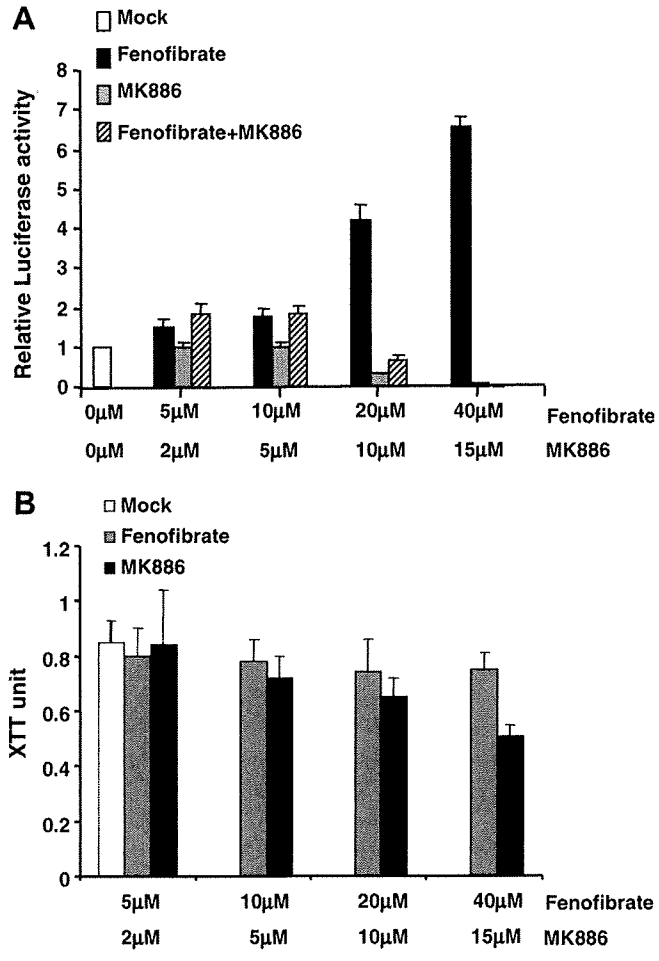

Fig. 4. The effects of PPARα agonists and antagonists on the replication of HCV subgenomic replicons. (A) LucNeo#2 cells containing a HCV subgenomic replicon termed LNMH14, were mock treated or treated with fenofibrate, MK886, or a combination of both fenofibrate and MK886 at the indicated concentrations for 2 days. Luciferase activity derived from the replicon was then measured as an indicator of HCV replication [7]. (B) Following treatment with fenofibrate and Mk886, LucNeo#2 cells were cultured for 2 days and cell viability measured using the XTT assay (Roche, Mannheim, Germany).

Discussion

In the current study, we demonstrated that immortalized hepatocyte HuS-E/2 cells cultured in 3D/TGP support the infection and replication of natural HCV derived from patient sera. Unlike recombinant HCVs, which have been required to adapt to sublines of HuH-7 cells [16], the population of the natural HCV is fairly polymorphic, demonstrating different responses to a variety of anti-viral agents [17,18]. The 3D/TGP-HuS-E/2 cells have the advantage of being a small-scale 3D cultured cells, which are cultured in 12-well plates at a density of 1×10^5/well, that allow the study of both viral and cellular events. In the current study, it demonstrated a 2 log increase in susceptibility to natural HCV infection and replication when compared to conventional 2D culture systems. Thus it offers an important advantage in the study of natural HCV infection and replication, and the response of natural HCV to anti-HCV drugs.

As the ability of HuS-E/2 cells to support infection and replication of natural HCV was greatly altered by the culture conditions, it is likely that the culture system described in our study will provide important information in regards to the cellular factors that support the HCV life cycle. The microarray study showed that the expression of some genes related to the PPARα signaling pathway were upregulated in the 3D cultured HuS-E/2 cells. Using both PPARα signaling agonists and antagonists, PPARα signaling was shown to affect infection and proliferation of natural HCV. PPARα is a ligand-activated transcription factor that is primarily expressed in tissues with high lipid metabolism including the liver, where it functions as one of three major nuclear receptors and is essential for its normal function [19]. Similar to a part of our data, a negative effect on HCV replication was previously observed in the replicon-bearing cells treated with siRNA for PPARα, with only 50% reduction of HCV-RNA [20]. In this study, even a large dose of PPARα agonist enhanced natural HCV replication in the 2D-HuS-E/2 cells for three times, despite the 2 logs enhancement of HCV proliferation in 3D/TGP culture. This implies that additional factors activated in 3D/TGP-HuS-E/2 cells may be required for the efficient HCV proliferation. Further analysis of the microarray data may provide us with further information on factors that may prove useful in the development of anti-HCV drugs.

In conclusion, the novel *in vitro* culture system combining TGP and immortalized hepatocytes described in this study demonstrated efficient support of natural HCV infection and replication. This system may be used in future virological studies to define new anti-HCV strategies. It may also prove useful for the specific design of effective individual therapy according to patient-specific strains.

Acknowledgments

This work was supported by Grants-in-Aid from the Ministry of Health, Labor and Welfare of Japan; and for scientific research from Ministry of Education, Sports, Culture, and Technology of Japan.

References

[1] Z. Younossi, J. Kallman, J. Kincaid, The effects of HCV infection and management on health-related quality of life, Hepatology 45 (2007) 806–816.

[2] M.W. Fried, M.L. Shiffman, K.R. Reddy, C. Smith, G. Marinos, F.L. Goncales Jr., D. Haussinger, M. Diago, G. Carosi, D. Dhumeaux, A. Craxi, A. Lin, J. Hoffman, J. Yu, Peginterferon alfa-2a plus ribavirin for chronic hepatitis C virus infection, N. Engl. J. Med. 347 (2002) 975–982.
[3] K. Murakami, K. Ishii, Y. Ishihara, S. Yoshizaki, K. Tanaka, Y. Gotoh, H. Aizaki, M. Kohara, H. Yoshioka, Y. Mori, N. Manabe, I. Shoji, T. Sata, R. Bartenschlager, Y. Matsuura, T. Miyamura, T. Suzuki, Production of infectious hepatitis C virus particles in three-dimensional cultures of the cell line carrying the genome-length dicistronic viral RNA of genotype 1b, Virology 351 (2006) 381–392.
[4] G. Andrei, Three-dimensional culture models for human viral diseases and antiviral drug development, Antiviral Res. 71 (2006) 96–107.
[5] H.H. Aly, K. Watashi, M. Hijikata, H. Kaneko, Y. Takada, H. Egawa, S. Uemoto, K. Shimotohno, Serum-derived hepatitis C virus infectivity in interferon regulatory factor-7-suppressed human primary hepatocytes, J. Hepatol. 46 (2007) 26–36.
[6] K. Goto, K. Watashi, T. Murata, T. Hishiki, M. Hijikata, K. Shimotohno, Evaluation of the anti-hepatitis C virus effects of cyclophilin inhibitors, cyclosporin A, and NIM811, Biochem. Biophys. Res. Commun. 343 (2006) 879–884.
[7] T. Murata, M. Hijikata, K. Shimotohno, Enhancement of internal ribosome entry site-mediated translation and replication of hepatitis C virus by PD98059, Virology 340 (2005) 105–115.
[8] M.A. El-Farrash, H.H. Aly, K. Watashi, M. Hijikata, H. Egawa, K. Shimotohno, In vitro infection of immortalized primary hepatocytes by HCV genotype 4a and inhibition of virus replication by cyclosporin, Microbiol. Immunol. 51 (2007) 127–133.
[9] J. Samulin, I. Berget, S. Lien, H. Sundvold, Differential gene expression of fatty acid binding proteins during porcine adipogenesis, Comp. Biochem. Physiol. B: Biochem. Mol. Biol. 151 (2008) 147–152.
[10] S. Hummasti, B.A. Laffitte, M.A. Watson, C. Galardi, L.C. Chao, L. Ramamurthy, J.T. Moore, P. Tontonoz, Liver X receptors are regulators of adipocyte gene expression but not differentiation: identification of apoD as a direct target, J. Lipid Res. 45 (2004) 616–625.
[11] C.G. Walker, M.J. Holness, G.F. Gibbons, M.C. Sugden, Fasting-induced increases in aquaporin 7 and adipose triglyceride lipase mRNA expression in adipose tissue are attenuated by peroxisome proliferator-activated receptor alpha deficiency, Int. J. Obes. (Lond.) 31 (2007) 1165–1171.
[12] D.G. Jump, D. Botolin, Y. Wang, J. Xu, B. Christian, O. Demeure, Fatty acid regulation of hepatic gene transcription, J. Nutr. 135 (2005) 2503–2506.
[13] D.W. Crabb, S. Liangpunsakul, Alcohol and lipid metabolism, J. Gastroenterol. Hepatol. 21 (Suppl. 3) (2006) S56–S60.
[14] D. Panigrahy, A. Kaipainen, S. Huang, C.E. Butterfield, C.M. Barnes, M. Fannon, A.M. Laforme, D.M. Chaponis, J. Folkman, M.W. Kieran, PPARalpha agonist fenofibrate suppresses tumor growth through direct and indirect angiogenesis inhibition, Proc. Natl. Acad. Sci. USA 105 (2008) 985–990.
[15] V.S. Deshpande, J.P. Kehrer, Mechanisms of *N*-acetylcysteine-driven enhancement of MK886-induced apoptosis, Cell Biol. Toxicol. 22 (2006) 303–311.
[16] K.J. Blight, A.A. Kolykhalov, C.M. Rice, Efficient initiation of HCV RNA replication in cell culture, Science 290 (2000) 1972–1974.
[17] R.C. Dickson, Clinical manifestations of hepatitis C, Clin. Liver Dis. 1 (1997) 569–585.
[18] E.J. Heathcote, Antiviral therapy: chronic hepatitis C, J. Viral Hepat. 14 (Suppl. 1) (2007) 82–88.
[19] C.N. Palmer, M.H. Hsu, K.J. Griffin, J.L. Raucy, E.F. Johnson, Peroxisome proliferator activated receptor-alpha expression in human liver, Mol. Pharmacol. 53 (1998) 14–22.
[20] B. Rakic, S.M. Sagan, M. Noestheden, S. Belanger, X. Nan, C.L. Evans, X.S. Xie, J.P. Pezacki, Peroxisome proliferator-activated receptor alpha antagonism inhibits hepatitis C virus replication, Chem. Biol. 13 (2006) 23–30.

THE JOURNAL OF BIOLOGICAL CHEMISTRY VOL. 284, NO. 12, pp. 8033–8041, March 20, 2009

TORC2, a Coactivator of cAMP-response Element-binding Protein, Promotes Epstein-Barr Virus Reactivation from Latency through Interaction with Viral BZLF1 Protein*[S]

Received for publication, November 6, 2008, and in revised form, January 21, 2009 Published, JBC Papers in Press, January 21, 2009, DOI 10.1074/jbc.M808466200

Takayuki Murata[‡], Yoshitaka Sato[‡1], Sanae Nakayama[‡], Ayumi Kudoh[‡1], Satoko Iwahori[‡], Hiroki Isomura[‡], Masako Tajima[§], Takayuki Hishiki[¶‖], Takayuki Ohshima[**], Makoto Hijikata[**], Kunitada Shimotohno[¶‖], and Tatsuya Tsurumi[‡2]

From the [‡]Division of Virology, Aichi Cancer Center Research Institute, 1-1, Kanokoden, Chikusa-ku, Nagoya 464-8681, [§]Central Clinical Laboratory, Teikyo University School of Medicine, Tokyo 173-0003, [¶]Research Institute, Chiba Institute of Technology, Narashino, Chiba 275-0016, [‖]Center for Integrated Medical Research, Keio University School of Medicine, Shinjuku, Tokyo 160-8582, and [**]Department of Viral Oncology, Institute for Virus Research, Kyoto University, Sakyo-ku, Kyoto 606-8507, Japan

Reactivation of the Epstein-Barr virus from latency is dependent on expression of the viral BZLF1 protein. The BZLF1 promoter (Zp) normally exhibits only low basal activity but is activated in response to chemical inducers such as 12-*O*-tetradecanoylphorbol-13-acetate and calcium ionophore. We found here that Transducer of Regulated cAMP-response Element-binding Protein (CREB) (TORC) 2 enhances Zp activity 10-fold and more than 100-fold with co-expression of the BZLF1 protein. Mutational analysis of Zp revealed that the activation by TORC is dependent on ZII and ZIII *cis* elements, binding sites for CREB family transcriptional factors and the BZLF1 protein, respectively. Immunoprecipitation, chromatin immunoprecipitation, and reporter assay using Gal4-luc and Gal4BD-BZLF1 fusion protein indicate that TORC2 interacts with BZLF1, and that the complex is efficiently recruited onto Zp. These observations clearly indicate that TORC2 activates the promoter through interaction with the BZLF1 protein as well as CREB family transcriptional factors. Induction of the lytic replication resulted in the translocation of TORC2 from cytoplasm to viral replication compartments in nuclei, and furthermore, activation of Zp by TORC2 was augmented by calcium-regulated phosphatase, calcineurin. Silencing of endogenous TORC2 gene expression by RNA interference decreased the levels of the BZLF1 protein in response to 12-*O*-tetradecanoylphorbol-13-acetate/ionophore. Based on these results, we conclude that Epstein-Barr virus exploits the calcineurin-TORC signaling pathway through interactions between TORC and the BZLF1 protein in reactivation from latency.

Epstein-Barr virus (EBV)[3] is a human γ-herpesvirus that predominantly establishes latent infection in B lymphocytes. Only a small percentage of infected cells switch from the latent stage into the lytic cycle and produce progeny viruses. Although the mechanism of EBV reactivation *in vivo* is not fully understood, it is known to be elicited by treatment of latently infected B cells with some chemical or biological reagents, such as 12-*O*-tetradecanoylphorbol-13-acetate (TPA), calcium ionophore, sodium butyrate, or immunoglobulin (Ig). Stimulation of the EBV lytic cascade by any of those reagents leads to the expression of two presumed viral immediate-early genes, BZLF1 and BRLF1. The BZLF1 protein is a transcriptional activator that shares structural similarities to the basic leucine zipper (b-Zip) family transcriptional factors, and BZLF1 expression alone can trigger the entire reactivation cascade (1–3).

Expression of the BZLF1 gene is tightly controlled at the transcriptional level. The BZLF1 promoter (Zp) normally exhibits low basal activity usually and is activated in response to TPA or the other reagents described above. The minimal sequence of Zp necessary for the activation by the inducers is 233 bp in length (4). The region harbors at least three types of *cis* regulatory elements, referred to as ZI, ZII, and ZIII. Four copies of the ZI element (ZIA-D) are distributed within the minimal Zp. The myocyte enhancer factor 2D binds to ZIA, ZIB, and ZID (5), whereas Sp1 or Sp3 can bind to ZIA, ZIC, and ZID (6). A single ZII element is located near TATA, sharing homology with binding sites for the cyclic AMP-response element-binding protein (CREB) or the AP-1 family transcriptional factor (7, 8). Two copies of the ZIII element (ZIIIA, B) are bound by the BZLF1 protein. Previous studies have demonstrated that both ZI and ZII elements are necessary for the initial activation of the promoter by TPA/ionophore or IgG(2). Then, the expressed BZLF1 protein joins to further activate Zp by binding to the ZIIIA and B elements (9).

* This work was supported by grants-In-aid for Scientific Research from Ministry of Education, Science, Sports, Culture, and Technology of Japan Grants 20012056, 19041078, and 20390137 (to T. T.) and 20790362 (to T. M.). The costs of publication of this article were defrayed in part by the payment of page charges. This article must therefore be hereby marked "*advertisement*" in accordance with 18 U.S.C. Section 1734 solely to indicate this fact.

[S] The on-line version of this article (available at http://www.jbc.org) contains supplemental Figs. S1–S4.

[1] Supported by a Research Fellowship of the Japanese Society for the Promotion of Science.

[2] To whom correspondence should be addressed. Tel. and Fax: 81-52-764-2979; E-mail: ttsurumi@aichi-cc.jp.

[3] The abbreviations used are: EBV, Epstein-Barr virus; Zp, BZLF1 promoter; CREB, cyclic AMP-response element (CRE)-binding protein; TORC, Transducer of Regulated CREB; TPA, 12-*O*-tetradecanoylphorbol-13-acetate; b-Zip, basic leucine zipper; CBP, CREB-binding protein; GAPDH, glyceraldehyde-3-phosphate dehydrogenase; IP, immunoprecipitation; IB, immunoblotting; ChIP, chromatin immunoprecipitation; siRNA, small interfering RNA; RT, reverse transcription; CMV, cytomegalovirus.

Transducer of Regulated CREB (TORC) 1, 2, and 3 were identified from a lymphocyte cDNA library as a family of CREB co-activators that bind to CREB and enhance CRE-mediated transcription in an Ser-133 phosphorylation-independent manner (10, 11). It was reported recently that TORCs are activated by the calcium-regulated phosphatase, calcineurin (12, 13). Dephosphorylation of TORC by the phosphatase triggers release from 14-3-3 proteins and translocation from cytoplasm to nucleus. Interestingly, the activation of EBV Zp is blocked by calcineurin inhibitors, such as cyclosporin A or FK506 (14). Based on these studies, we hypothesized that TORCs might be involved in the transcriptional activation of Zp, leading to a switch from latent state to the lytic replication.

In the present study we show that TORC1, -2, and -3 can all enhance Zp, especially with co-expression of BZLF1. TORCs activate the promoter through interaction not only with CREB but also the BZLF1 protein. We also provide evidence that the activation of the promoter by TORC2 is up-regulated by calcium-regulated phosphatase, calcineurin. These results indicate involvement of TORCs in EBV reactivation from latency.

EXPERIMENTAL PROCEDURES

Cell Culture and Antibodies—HEK293T, EBV-Bac-293, and GTC-4 cells were maintained in Dulbecco's modified Eagle's medium (Invitrogen) supplemented with 10% fetal bovine serum. EBV-293 cells were prepared by transfection with EBV-Bac DNA (15) into HEK293 cells subcloned in our laboratory (16) followed by hygromycin selection. GTC-4 is a cell line established from an EBV-positive gastric cancer by Dr. M. Tajima (Teikyo University) (17). Akata, B95-8, and Tet-BZLF1/B95-8 cells were maintained in RPMI1640 as described previously (18, 19). To induce lytic EBV replication in Tet-BZLF1/B95-8 cells, a tetracycline derivative, doxycycline, was added to the culture medium at a final concentration of 2 μg/ml. The mouse anti-FLAG, hemagglutinin, -BZLF1, and -GAPDH antibodies were from Sigma, Roche Applied Science, Dako A/S, and Ambion, respectively. Rabbit anti-PCNA and -TORC2 antibodies were from Oncogene and Calbiochem, respectively, and rabbit anti-BMRF1 and -BALF5 antibodies have been reported previously (20). The anti-tubulin antibody was purchased from Cell Signaling. Horseradish peroxidase-linked goat antibodies to mouse or rabbit IgG were from Amersham Biosciences. Horseradish peroxidase (HRP)-linked goat antibody to rat IgG was obtained from Jackson ImmunoResearch, and TrueBlot HRP anti-mouse and rabbit IgG were from eBioscience.

Plasmid Construction—The pZp-luc reporter plasmid was constructed by inserting the minimal sequence of Zp (from −221 to +12) prepared by PCR into XhoI and HindIII sites of pGL4.10 (Promega). Primer sequences for the PCR were 5′-TAGCCTCGAGGCCATGCATATTTCAACTGG-3′ (forward), 5′-GCCAAGCTTCAAGGTGCAATGTTTAGTGAG-3′ (reverse). Point mutations in the minimal Zp were introduced by PCR using following primers: mZII, 5′-TCACAGAGGAGGCTGGTGCC-3′ (forward), 5′-TGAATTCGTTTGGGACGTGC-3′ (reverse); mZIII, 5′-GCACCGCTAATGTACCTCATAG-3′ (forward), 5′-CTGTGAATTCTGCATAGTTTC-3′ (reverse). Expression plasmids for TORC3 and CREB1A have been reported elsewhere (21–23). TORC1 and TORC2 genes were amplified and cloned into EcoRI and XhoI sites of pcHA (22, 24) using the following primers: TORC1, 5′-AAAGAATTCATGGCGACTTCGAACAATCCGCGG-3′ (forward), 5′-AAACTCGAGTCACAGGCGGTCCATCCGGAAGGT-3′ (reverse), TORC2, 5′-AAAGAATTCATGGCGACGTCGGGGGCGAACGGG-3′ (forward), 5′-AAACTCGAGTCATTGGAGCCGGTCACTGCGGAA-3′ (reverse). The pCRE-Luc and pRL-TK reporter plasmids were obtained commercially (Stratagene). For the pcDNABZLF1 expression plasmid, the BZLF1 gene was cloned into pcDNA3 at BamHI and XhoI sites. The sequence in the b-Zip domain (amino acids 200–227) was deleted to generate pcDNAdBZLF1. To prepare the expression vector for Gal4-BZLF1fusion protein, the BZLF1 sequence was recloned into EcoRI and XbaI sites of the pM vector (Clontech) after PCR using the primers 5′-CCGGAATTCATGATGGACCCAAACTCGAC-3′ (forward) and 5′-CTTATCTAGATTAGAAATTTAAGAGATCCTCG-3′ (reverse). The pGal4-luc reporter plasmid has been reported previously (21).

Transfection and Luciferase Assay—Plasmid DNA was transfected into HEK293T or EBV-293 cells using Lipofectamine 2000 reagent (Invitrogen). The total amounts of plasmid DNAs were standardized by the addition of an empty vector, pcDNA3. Proteins were extracted from cells with the lysis buffer supplied in a Dual Luciferase Reporter Assay System (Promega) kit, and luciferase activities were measured using the kit. The counts for firefly luciferase were normalized to those for renilla luciferase. GTC-4 and Akata cells were electronically transfected using a Microporator (Digital Bio).

Immunoprecipitation (IP) and Immunoblotting (IB)—For IP, cells were lysed in 0.2% Nonidet P-40 buffer (10 mM Tris-HCl, pH 7.8, 100 mM NaCl, 1 mM EDTA, 0.1% Nonidet P-40, and protease and phosphatase inhibitor mixture). After centrifugation, lysates were precleared with protein G-Sepharose (Amersham Biosciences), mixed with antibody, and then incubated for 1 h. Immunocomplexes were recovered by incubating with G-Sepharose for 1 h, and the resin was washed 5 times with the same buffer. Samples were subjected to SDS-PAGE followed by IB with the indicated antibodies as described previously (24).

Chromatin IP (ChIP) Assay—ChIP assays were performed essentially as described (Upstate Biotechnology, Inc.) with formaldehyde cross-linked chromatin from 1×10^6 cells for each reaction. Cells were lysed, and chromatin was sonicated to obtain DNA fragments with an average length of 300 bp. After centrifugation, the chromatin was diluted 10-fold with ChIP dilution buffer and precleared with protein A-agarose beads containing salmon sperm DNA (Upstate). Anti-FLAG IgG or normal rabbit IgG were added to the sample and incubated overnight with rotation. The immune complexes were collected by the addition of the protein A-agarose beads, and DNA was purified using a QIAquick PCR purification kit (Qiagen) after uncoupling of the cross-linking and proteinase K digestion. The recovered DNA was amplified by PCR using primers specific for Zp, 5′-TAGCCTCGAGGCCATGCATATTTCAACTGG-3′ and 5′-GCCAAGCTTCAAGGTGCAATGTTTAGTGAG-3′, and for the EBNA-1 open reading frame, 5′-GTCATCATCATCCGGGTCTC-3′ and 5′-TTCGGGTTGGAACCTCCTTG-3′. The PCR products were then analyzed

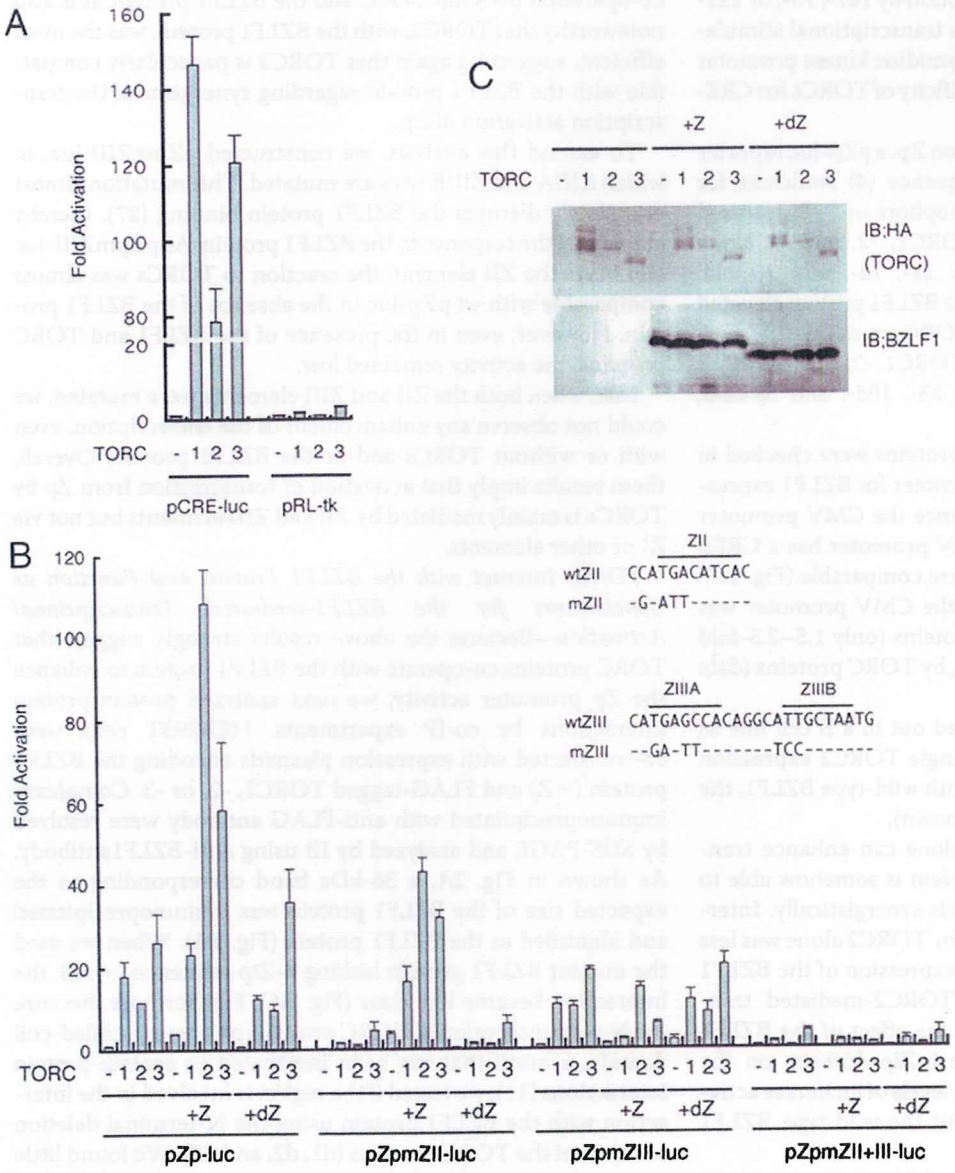

FIGURE 1. **TORCs activate transcription from Zp.** *A*, TORCs enhance CRE-dependent transcription. HEK293T cells were transfected with 10 ng of pCRE-luc or pRL-TK reporter plasmid and 50 ng of expression plasmids for TORC1, -2, or -3. Luciferase assays were carried out as described under "Experimental Procedures." The luciferase activity is shown as –fold activation of that without TORC for each reporter. *B*, effects of TORC proteins on Zp. HEK293 cells were transfected with 10 ng of reporter plasmid, pZp-luc, or its derivatives and 50 ng of expression plasmids for TORC1, -2, or -3 with 10 ng pcDNABZLF1 (+*Z*) or pcDNAdBZLF1 (+*dZ*) lacking b-Zip domain. The pZp-luc reporter contains the minimal Zp for the EBV B95-8 strain. For derivatives, specific mutations were introduced for mZII or/and mZIII as indicated. Luciferase assays were carried out as described under "Experimental Procedures." The luciferase activity is shown as -fold activation of that with neither BZLF1 nor TORC for pZp-luc (*leftmost bar*). Each *bar* represents the mean and S.D. of three independent transfections. *wt*, wild type. *C*, the expression levels of TORC and BZLF1 proteins in *B* were measured by immunoblotting.

by agarose gel electrophoresis and visualized with ethidium bromide staining.

Immunofluorescence Assay—For HEK293 cells, cells were fixed with 1% formaldehyde and permeabilized with 0.1% Nonidet P-40 in phosphate-buffered saline. The cells were washed and blocked in 1% bovine serum albumin in phosphate-buffered saline and then incubated with anti-FLAG antibody. Samples were then incubated with the secondary goat anti-mouse IgG antibody conjugated with Alexa Fluor 488. For Tet-BZLF1/B95-8, staining was carried out as described (25). Briefly, cells were washed with phosphate-buffered saline and lysed in ice-cold 0.5% Triton X-100-mCSK buffer (10 mM PIPES (pH 6.8), 100 mM NaCl, 300 mM sucrose, 1 mM $MgCl_2$, 1 mM EDTA, 1 mM dithiothreitol, 0.5% Triton X-100, and protease inhibitors) and fixed with 70% ethanol. The cells were blocked and then incubated overnight with primary antibodies. The samples were then incubated for 2 h with the secondary goat anti-mouse and rabbit IgG antibodies conjugated with Alexa Fluor 488 and 594, respectively. After immunostaining, cells were then mounted and stained with 4′,6-diamidino-2-phenylindole (DAPI) using ProLong Gold antifade reagent with DAPI (Invitrogen). Image acquisition was performed with a Bio-Rad Radiance 2000 confocal laser-scanning microscope equipped with a PlainApo 100 × 1.4-numerical-aperture oil immersion objective lens.

Small Interfering RNA (siRNA) and RT-PCR—Duplexes of 21-nucleotide (siRNA) specific to TORC2 mRNA, including two nucleotides of deoxythymidine at the 3′ end, were synthesized and annealed (Sigma Genosys). The sense and antisense sequences of the duplex were 5′-CUGCGACUGGCAUACACAAdTdT-3′ and 5′-UUGUGUAUGCCAGUCGCAGdTdT-3′, respectively. GTC-4 or Akata cells (1×10^5) were transfected with 50 pmol of the duplex RNA per well of a 24-well plate using a Microporator (Digital Bio). Twenty-four hours after transfection, TPA and A23187 or IgG were added and then incubated for another 24 h. Cells were then harvested for RT-PCR and IB. Primers used for the RT-PCR were as follows: for TORC2 mRNA, 5′-AAAGAATTCTACACAAGGAGCTCTCATTATG-3′ and 5′-GCTTGTCCTGTTAAGTGCAG-3′; for GAPDH mRNA, 5′-GGGAAGGTGAAGGTCGGAGT-3′ and 5′-AAGACGCCAGTGGACTCCAC-3′.

RESULTS

TORC Activates Transcription from EBV Zp—To confirm that TORC proteins activate CRE-dependent transcription, luciferase assays using pCRE-luc and pRL-TK reporter vectors were performed (Fig. 1*A*). Expression of TORC1, -2, or -3

enhanced the CRE-mediated transcription by 147-, 79-, or 121-fold, respectively, whereas no obvious transcriptional stimulation from the herpes simplex virus thymidine kinase promoter was observed, demonstrating the specificity of TORCs for CRE-dependent transcription.

To test the effect of TORC proteins on Zp, a pZp-luc reporter plasmid containing the minimal sequence (4) sufficient for transcriptional activation by TPA/ionophore or IgG was used for the assay. It was found that TORC1, -2, and -3 alone enhanced transcription from Zp by 18-, 12-, and 26-fold, respectively (Fig. 1*B*). Expression of the BZLF1 protein elevated the transcription in the absence of TORC up to 3.9-fold. Co-expression of the BZLF1 protein and TORC1, -2, and -3 further enhanced pZp-luc activity, reaching 23-, 108-, and 58-fold, respectively.

Levels of BZLF1 as well as TORC proteins were checked in Fig. 1*C* because we used the CMV promoter for BZLF1 expression, and TORC proteins might enhance the CMV promoter activity. Despite the fact that the CMV promoter has a CREB binding motif (26), levels of BZLF1 were comparable (Fig. 1*C*). A reporter assay also indicated that the CMV promoter was only marginally affected by TORC proteins (only 1.5–2.5-fold increase), at least under this condition, by TORC proteins (data not shown).

Analogous experiments were carried out in a B cell line as well (data not shown). In B cells, a single TORC2 expression caused a 9.9-fold enhancement, and with wild-type BZLF1, the activity reached to 48-fold (data not shown).

Taken together, although TORC alone can enhance transcription from the Zp, the BZLF1 protein is somehow able to further increase the transcription levels synergistically. Interestingly, although the activation of Zp by TORC2 alone was less potent than that by TORC1 or -3, co-expression of the BZLF1 protein dramatically enhanced the TORC2-mediated transcriptional activation. We also tested the effect of the BZLF1 deletion mutant dZ, which lacks the b-Zip domain, on the reporter gene as negative controls. The levels of luciferase activity were almost equal to those without the wild-type BZLF1 protein.

To further analyze the synergistic enforcement of Zp by TORCs, a pZpmZII-luc plasmid was made, the ZII element being mutated as shown in Fig. 1*B*. This mutation disrupts the CRE/activation transcription factor motif and abrogates the induction from the promoter by TPA/ionophore or IgG (4). The basal luciferase activity from this reporter plasmid became very low (only 25% of wt pZp-luc), and the activity did not appreciably increase even with TORC proteins (Fig. 1*B*), showing that the Zp activation by TORCs in the absence of the BZLF1 protein is caused through the ZII domain containing the CRE/activation transcription factor motif. However, this reporter still responded to the BZLF1 expression, reaching the same levels of transcriptional activity as with wt pZp-luc because it still contained ZIII, the BZLF1 protein binding sites. When TORC1, -2, or -3 were co-expressed with the BZLF1 protein, pZpmZII-luc exhibited significant enhancement of the transcriptional activity to around 20–50-fold. Because TORCs could not enhance this mutant promoter activity without expression of the BZLF1 protein, this activation might be due to co-operation between TORC and the BZLF1 protein. It is also noteworthy that TORC2, with the BZLF1 protein, was the most efficient, suggesting again that TORC2 is particularly compatible with the BZLF1 protein regarding synergism of the transcription activation of Zp.

To extend this analysis, we constructed pZpmZIII-luc, in which ZIIIA and ZIIIB sites are mutated. This mutation almost completely disrupts the BZLF1 protein binding (27), thereby abolishing the response to the BZLF1 protein. As pZpmZIII-luc still bears the ZII element, the reaction to TORCs was almost comparable with wt pZp-luc in the absence of the BZLF1 protein. However, even in the presence of the BZLF1 and TORC proteins, the activity remained low.

Last, when both the ZII and ZIII elements were mutated, we could not observe any enhancement of the transcription, even with or without TORCs and/or the BZLF1 protein. Overall, these results imply that activation of transcription from Zp by TORCs is mainly mediated by ZII and ZIII elements but not via ZI or other elements.

TORCs Interact with the BZLF1 Protein and Function as Coactivators for the BZLF1-mediated Transcriptional Activation—Because the above results strongly suggest that TORC proteins co-operate with the BZLF1 protein to enhance the Zp promoter activity, we next analyzed protein-protein interactions by co-IP experiments. HEK293T cells were co-transfected with expression plasmids encoding the BZLF1 protein (+Z) and FLAG-tagged TORC1, -2, or -3. Complexes immunoprecipitated with anti-FLAG antibody were resolved by SDS-PAGE and analyzed by IB using anti-BZLF1antibody. As shown in Fig. 2*A*, a 36-kDa band corresponding to the expected size of the BZLF1 protein was immunoprecipitated and identified as the BZLF1 protein (Fig. 2*A*). When we used the mutant BZLF1 protein lacking b-Zip sequence (+dZ), the interaction became less clear (Fig. 2*A*). Furthermore, because the N-terminal region of TORC proteins possesses a coiled-coil domain, a motif that has been implicated in protein-protein interactions (11), we tested if the region is involved in the interaction with the BZLF1 protein using the N-terminal deletion mutants of the TORC proteins (d1, d2, and d3). We found little or no association of the TORC mutants with the BZLF1 protein in the absence of the coiled-coil domain (Fig. 2*A*).

To examine whether TORC proteins have effects on BZLF1 protein-dependent transcriptional activity, we prepared an expression plasmid encoding a Gal4 DNA binding domain-BZLF1 fusion protein (Gal4-Z) and pGal4-luc, which contains five Gal4 binding sites and an SV40 minimal promoter. Expression of Gal4-BZLF1 fusion protein alone was able to activate pGal4-luc 3.6-fold (Fig. 2*B*). Because binding between the polypeptide of Gal4 DNA binding domain and the Gal4 binding sites in the promoter of the reporter construct is highly specific and exclusive, only the Gal4-BZLF1 fusion protein can be recruited onto the promoter, indicating that the increase reflects the net transcriptional activity of the BZLF1 protein but not of any other factors. Co-expression of Gal4-BZLF1 and TORC1, -2, and -3 proteins resulted in an 14-, 8.0-, and 9.9-fold increase, respectively, in the transcriptional activity as compared with Gal4-BZLF1 alone, whereas deletion mutants of the TORC proteins (d1, d2, and d3) failed to increase the levels

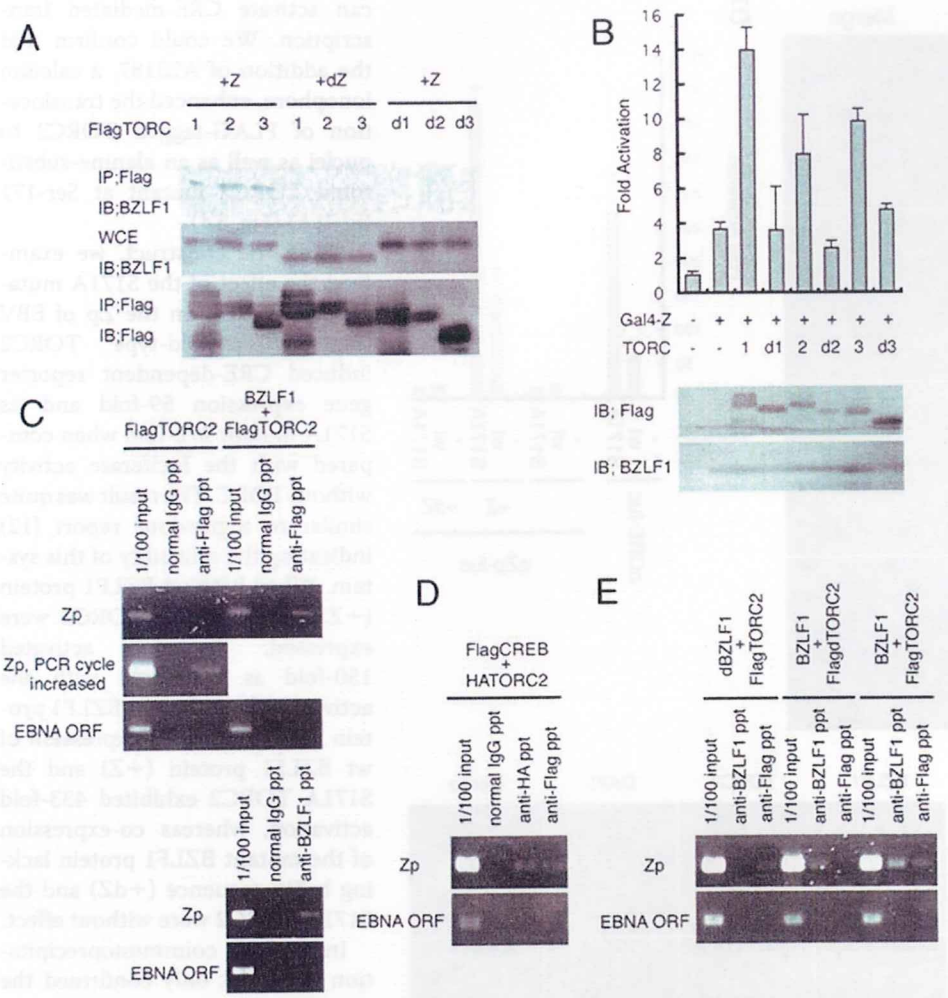

FIGURE 2. **TORCs associate with the BZLF1 protein to enhance transcription from Zp.** *A*, TORCs coimmunoprecipitated with the BZLF1 protein. FLAG-tagged TORC1, 2-, -3 or FLAG-tagged TORC with deletion at the coiled-coil domain of the protein (*d1*, *d2*, *d3*) expression vectors were co-transfected with wt BZLF1 (+*Z*) or BZLF1 without the b-Zip (+*dZ*) expression vector. IP was carried out using anti-FLAG antibody and immunoblotted with anti-BZLF1 antibody (*top*), then stripped and reprobed with anti-FLAG antibody (*bottom*). As a control, whole cell extracts (*WCE*) from the samples were also stained with anti-BZLF1 antibody (*middle*). *B*, BZLF1 protein-dependent transcription is enhanced by TORCs. HEK293T cells were transfected with 25 ng of Gal4-luciferase reporter plasmid and 25 ng of the plasmid expressing the Gal4 DNA binding domain-BZLF1 fusion protein (+*Gal4-Z*) together with 100 ng of plasmids expressing TORC1, 2-, -3 or the deletion mutant at the coiled-coil domain (*d1*, *d2*, *d3*). Luciferase assays were carried out as described under "Experimental Procedures." The luciferase activity is shown as -fold activation of that with neither Gal4-Z nor TORC. Each *bar* represents the mean and S.D. of three independent transfections. Expression levels of FLAG-tagged TORC proteins and BZLF1 were also analyzed. *C*, ChIP assays were performed to evaluate the association of TORC2 with Zp. EBV-293cells were transfected with a FLAG-tagged TORC2 expression plasmid with or without the BZLF1 expression plasmid. After fixation and sonication, protein-DNA complexes were immunoprecipitated with anti-FLAG (*upper panels*) or anti-BZLF1 (*lower panels*) antibody or normal IgG followed by uncoupling of the cross-linking and PCR reactions using primers for Zp or the coding region of EBNA-1. *ORF*, open reading frame; *ppt*, precipitate. *D*, ChIP assays were carried out to show that both CREB and TORC2 were recruited to the Zp even without BZLF1. EBV-293cells transfected with FLAG-tagged CREB and hemagglutinin-tagged TORC2 expression vectors were subjected to ChIP assay with normal IgG, anti-hemagglutinin (*HA*), or -FLAG antibody followed by PCR. *E*, ChIP assays showing the importance of b-Zip of BZLF1 and coiled-coil domain of TORC2 for their recruitment to the promoter. Wild-type or deletion mutant of BZLF1 and FLAG-tagged TORC2 were transfected in pairs as noted. Precipitations were done using the anti-BZLF1 or -FLAG antibody followed by detection.

(3.5-, 2.5-, and 4.7-fold, respectively). This induction of the luciferase activity means that TORC functions through the BZLF1 protein but not through any other factors, as the only protein on the promoter is Gal4-BZLF1.

To further analyze the behavior of TORC on the Zp promoter, we checked whether TORC was recruited onto the Zp *in vivo* by ChIP assays (Fig. 2*C*). We used TORC2 because it has been studied most extensively and was demonstrated to be the most crucial factor, at least *in vivo* (28–31) (also see Figs. 1, 4, and 5). EBV-293 cells harboring EBV Bac DNA were transfected with the expression plasmid of FLAG-tagged TORC2 with or without the BZLF1 expression vector, and then ChIP assays were performed using the anti-FLAG antibody and normal IgG as a negative control. With expression of the BZLF1 protein, FLAG-tagged TORC2 was recruited to the Zp of the EBV genome in cells (Fig. 2*C*, *top panel*, *right*). In contrast, TORC2 was hardly detected without BZLF1 on the promoter (Fig. 2*C*, *top panel*, *left*) unless the PCR cycle was increased (Fig. 2*C*, *second panel*). A primer set for the EBNA-1 coding region was included (Fig. 2*C*, *third panel*) as a negative control to prove that the signal for the Zp was specific. We also confirmed that the BZLF1 protein was also recruited to the Zp when both the BZLF1 protein and FLAG-tagged TORC2 were expressed (Fig. 2*C*, *fourth panel*).

In the *second panel* in Fig. 2*C*, TORC2 was shown to be recruited onto Zp without BZLF1. Speculating that TORC2 is on the promoter through the interaction with CREB, the association of CREB protein with the promoter was also tested in Fig. 2*D*. As expected, both CREB and TORC2 came onto Zp even without BZLF1 protein.

To further confirm the importance of the interaction between BZLF1 and TORC2, we also tested dBZLF1, which lacks the b-Zip motif, and dTORC2, which is devoid of coiled-coil motif (Fig. 2*E*). When wild-type BZLF1 and wild-type TORC2 were present, both were detected bound to Zp (Fig. 2*E*, *right*). Deletion of the coiled-coil domain in TORC2 caused significant loss of its binding (Fig. 2*E*, *middle*), and truncation of BZLF1 b-Zip also harmed its association with Zp (Fig. 2*E*, *left*).

Activation of TORC2 by Dephosphorylation and Nuclear Transport—It has been demonstrated that the phosphorylation state of TORC2 regulates its activity (12, 13). Under normal conditions, TORC2 is sequestered by cytoplasmic 14-3-3 proteins, which recognize phosphorylated proteins. In the pres-

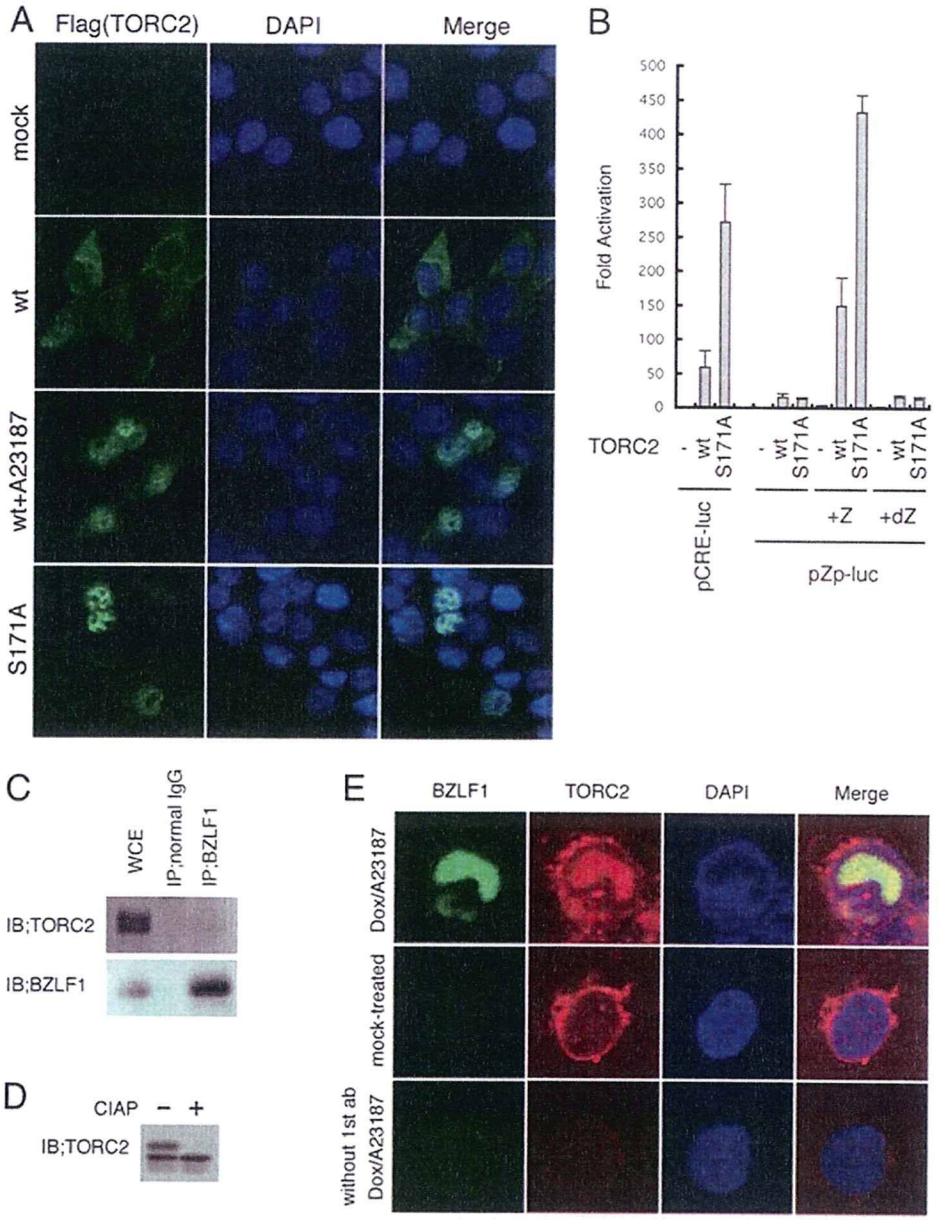

FIGURE 3. **Dephosphorylation of TORC2 at Ser171 promotes nuclear localization and transcriptional activation for Zp.** *A*, immunocytochemical analysis showing the effects of ionophore (A23187) or the S171A mutation of TORC2 on its subcellular localization. Cells were stained with anti-FLAG antibody (*green*) and 4′,6-diamidino-2-phenylindole (*DAPI*; *blue*). *wt*, wild type. *B*, transient reporter assay results for the CRE-mediated promoter (*left*) and Zp (*right*). HEK293T cells were transfected with pCRE-luc or pZp-luc together with expression vectors for the wild-type or the S171A mutant of TORC2. For pZp-luc, plasmids with wt BZLF1 (+*Z*) or a mutant BZLF1 lacking the b-Zip domain (+*dZ*) were also transfected. Luciferase assays were carried out as described under "Experimental Procedures." The luciferase activity is shown as -fold activation of that without TORC2 for pCRE-luc (*left part*) and that with neither BZLF1 nor TORC2 for pZp-luc (*right*). Each *bar* represents the mean and S.D. of three independent transfections. *C*, dephosphorylated TORC2 interacts with BZLF1. Protein lysates from B95-8 cells treated with TPA and A23187 for 24 h were subjected to IP using normal IgG or anti-BZLF1 antibody followed by SDS-PAGE and IB with anti-TORC2 (*upper panel*) and -BZLF1 (*lower panel*) antibodies. *WCE*, whole cell extracts. *D*, phosphorylation of TORC2. Proteins from B95-8 cells treated with TPA and A23187 were lysed in calf intestine alkaline phosphatase buffer and incubated with or without calf intestine alkaline phosphatase for 1h followed by SDS-PAGE and IB with anti-TORC2 antibody. *E*, localization of endogenous TORC2 (*red*) and BZLF1 protein (*green*) in Tet-BZLF1/B95-8 cells. Cells were mock-treated (*middle panels*) or treated with doxycycline and A23187 (*top* and *bottom panels*) and analyzed by immunofluorescence assay using confocal microscopy. 4′,6-Diamidino-2-phenylindole (*blue*) staining was also carried out. As a negative control, treatment with first antibodies was omitted for the *bottom panels*.

ence of calcium signaling, TORC2 is dephosphorylated by calcineurin at phosphoserine 171, triggering disruption of the interaction with 14-3-3 and import into the nucleus where it can activate CRE-mediated transcription. We could confirm that the addition of A23187, a calcium ionophore, enhanced the translocation of FLAG-tagged TORC2 to nuclei as well as an alanine-substituted TORC2 mutant at Ser-171 (S171A) (Fig. 3*A*).

Using the construct, we examined the effect of the S171A mutation of TORC2 on the Zp of EBV (Fig. 3*B*). Wild-type TORC2 induced CRE-dependent reporter gene expression 59-fold and its S171A mutant 272-fold when compared with the luciferase activity without TORC. The result was quite similar to a previous report (12) indicating the reliability of this system. When both wt BZLF1 protein (+Z) and wild-type TORC2 were expressed, Zp was activated 150-fold as compared with the activity with neither wt BZLF1 protein nor TORC2. Co-expression of wt BZLF1 protein (+Z) and the S171A TORC2 exhibited 433-fold activation, whereas co-expression of the mutant BZLF1 protein lacking b-Zip sequence (+dZ) and the S171A TORC2 were without effect.

In Fig. 3*C*, coimmunoprecipitation assay not only confirmed the interaction between endogenous TORC2 and BZLF1 but also revealed that BZLF1 protein preferentially associates with faster-migrating species of TORC2, which are dephosphorylated forms of the protein (Fig. 3*D*) (12, 31).

In the EBV lytic replication, it was previously demonstrated that the BZLF1 protein localizes to replication compartments, the sites of viral genome replication and transcription, in the nuclei (3, 32). Immunofluorescence analysis showed that upon induction, TORC2 was recruited to the replication compartments and colocalized with BZLF1 protein in the nucleus in the lytic phase, whereas the protein was localized in the cytoplasm in the latent phase (Fig. 3*E*).

In addition, we confirmed that cyclosporin A, an inhibitor of calcineurin signaling pathway, clearly blocks the BZLF1 expression in B95-8 cells treated with TPA and calcium ionophore (supplemental Fig. S1). These results

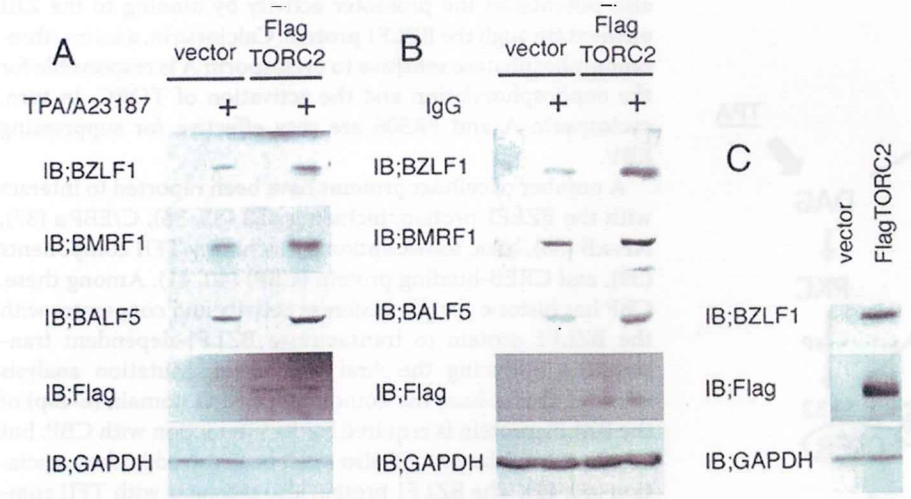

FIGURE 4. **Increased expression of the BZLF1 protein on exogenous expression of TORC2.** *A* and *B*, GTC-4 (*A*) cells or Akata (*B*) cells were transfected with the TORC2 expression vector, and 24 h thereafter, TPA(20 ng/ml) and A23187 (0.5 μM) or IgG was added to the culture followed by incubation for another 24 h and IB with anti-BZLF1, -BMRF1, -BALF5, -FLAG, and -GAPDH antibodies. *C*, EBV-293 cells transfected with the TORC2 expression vector were incubated for 24 h followed by IB with anti-BZLF1, -FLAG, and -GAPDH antibodies.

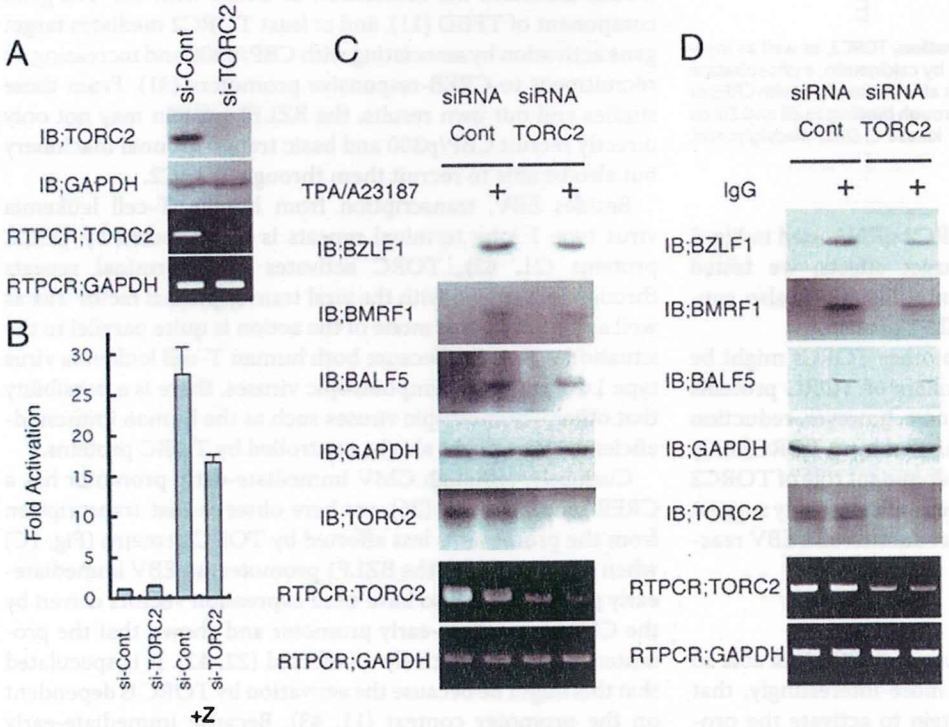

FIGURE 5. **BZLF1-mediated transcription depends on endogenous TORC2 expression.** *A* and *B*, HEK293T cells were transfected with duplexes of 21-nucleotide siRNA against TORC2 (*si-TORC2*) or control (*si-Cont*) siRNA together with 10 ng of pZp-luc with or without 10 ng pcDNABZLF1 (+*Z*). IB and RT-PCR assays (*A*) and luciferase assays (*B*) were carried out as described under "Experimental Procedures." The luciferase activity is shown as -fold activation of that with control siRNA without BZLF1. Each *bar* represents the mean and S.D. of three independent transfections. *C* and *D*, knock-down of TORC2 mRNA in GTC-4 (*C*) and Akata (*D*) cells. Cells transfected with siRNA against TORC2 (*siRNA TORC2*) or the Control (*siRNA Cont*) were cultured with TPA (20 ng/ml) and A23187 (0.5 μM) or IgG for 24 h. Protein or mRNA levels of BZLF1, BMRF1, BALF5, TORC2, and GAPDH were examined by IB or RT-PCR.

suggest a cooperative influence of the BZLF1 protein and dephosphorylated TORC2 in the presence of calcineurin signaling activation.

Role of TORC2 in EBV Reactivation from Latency—To examine the role of TORC2 in EBV reactivation from latency, GTC-4 cells, in which EBV is latently infected, were transfected with the TORC2 expression vector and incubated with or without TPA/A23187 (Fig. 4*A*). The cells expressed the BZLF1, BMRF1, and BALF5 proteins in response to TPA/A23187 treatment, and further exogenous expression of TORC2 increased the levels of the proteins. A similar result was obtained in Akata cells (Fig. 4*B*). Expression of S171A mutant of TORC2 appears to impact on BZLF1 levels significantly (data not shown). We also tested EBV-293 cells, in which levels of exogenous gene expression are very efficient (Fig. 4*C*). Even in the absence of TPA/A23187, overexpression of TORC2 clearly enhanced BZLF1 protein levels.

To examine the function of TORC2 under physiological conditions, we employed siRNA technology using a synthetic oligonucleotide that forms a duplex RNA encoding partial nucleotides from TORC2. As shown in Fig. 5*A*, treatment with siRNA against TORC2 reduced the level of TORC2 mRNA in HEK293T cells, whereas the level of GAPDH remained unchanged. TORC2 siRNA treatment also resulted in a decrease in the BZLF1-mediated transcription (Fig. 5*B*; +*Z*, *si-TORC2*) when compared with control siRNA treatment (+*Z*, *si-Cont*).

In addition, the effect of siRNA against TORC2 was also examined in GTC-4 and Akata cells, as shown in Fig. 5, *C* and *D*, respectively. Treatment with TORC2 siRNA suppressed the mRNA expression of TORC2, whereas the GAPDH gene was unaffected. The treatment also reduced the levels of viral lytic proteins including BZLF1.

To eliminate the possibility that the siRNA against TORC2 might elicit interferon signaling pathway, we analyzed interferon-β expression by RT-PCR (33) because activation of the signaling pathway provoked by double-stranded RNA causes the promoter activation. Treatment with TORC2 siRNA did not induce the levels of interferon-β (supplemental Fig. S2), indicating that interferon signaling is not activated by si-TORC2.

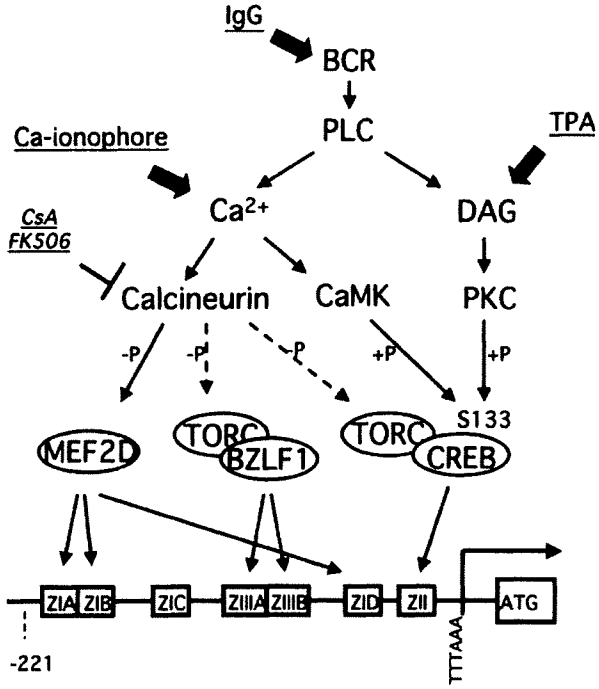

FIGURE 6. **Proposed model for EBV Zp activation.** TORC2, as well as myocyte enhancer factor 2D (*MEF2D*), is activated by calcineurin, a phosphatase that can be inhibited by CsA or FK506. TORC2 is able to associate with CREB or the BZLF1 protein and enhances Zp activity through binding to ZII and ZIII *cis* elements. *PLC*, phospholipase C; *PKC*, protein kinase C; *DAG*, diacylglycerol; *CaM*, calmodulin; BCR, B-cell receptor.

To deny the possibility that the TORC2 siRNA used in Fig. 5 might act through unknown off-target effects, we tested another TORC2 siRNA in supplemental Fig. S3. It also suppressed the expression level of the BZLF1 protein.

To test if not only TORC2 but also other TORCs might be involved in this process, all the members of TORC proteins were silenced simultaneously. In that case, however, reduction of the BZLF1 level was no stronger than that by si-TORC2 only (Fig. supplemental S4), suggesting the dominant role of TORC2 in this transcriptional activation. These results strongly suggest the importance of TORC2 in BZLF1 production and EBV reactivation from latency.

DISCUSSION

In this report we document evidence that TORC is able to enhance transcription from Zp and, more interestingly, that TORC interacts with the BZLF1 protein to activate the promoter very strongly. Fig. 6 shows our working model for Zp induction. Previous studies have demonstrated that both ZI and ZII elements are necessary for the initial activation (2, 34). It has been reported that myocyte enhancer factor 2D plays a crucial role in virus reactivation from latency (5), being dephosphorylated by calcineurin and enhancing its binding to ZI. CREB family transcription factors bind to ZII when phosphorylated by protein kinase C, calmodulin kinase, or possibly mitogen-activated protein kinases. In addition to the activation by phosphorylation, our reporter assays indicated that CREB is activated by TORC in a CREB phosphorylation-independent manner. Furthermore, our study strongly suggests that TORC also potentiates the promoter activity by binding to the ZIII element through the BZLF1 protein. Calcineurin, a serine/threonine-phosphatase sensitive to cyclosporin A is responsible for the dephosphorylation and the activation of TORC. In turn, cyclosporin A and FK506 are very effective for suppressing EBV.

A number of cellular proteins have been reported to interact with the BZLF1 protein, including p53 (35, 36), C/EBPα (37), NF-κB (38), basic transcriptional machinery TFII components (39), and CREB-binding protein (CBP) (40, 41). Among these, CBP has histone acetyltransferase activity and cooperates with the BZLF1 protein to transactivate BZLF1-dependent transcription, inducing the viral lytic cycle. Mutation analysis revealed that at least the homodimerization domain (b-Zip) of the BZLF1 protein is required for its interaction with CBP, but other parts of the protein also must be involved in the association (40, 41). The BZLF1 protein also interacts with TFII components mainly through the transactivation domain and stabilizes the association of initiation complexes on DNA. Stable assembly of general transcriptional machinery might promote transcription from BZLF1-responsive promoters. Interestingly, TORC enhances the interaction of CREB with the $TAF_{II}130$ component of TFIID (11), and at least TORC2 mediates target gene activation by associating with CBP/p300 and increasing its recruitment to CREB-responsive promoters (31). From these studies and our own results, the BZLF1 protein may not only directly recruit CBP/p300 and basic transcriptional machinery but also be able to recruit them through TORC2.

Besides EBV, transcription from human T-cell leukemia virus type 1 long terminal repeats is also affected by TORC proteins (21, 42). TORC activates long terminal repeats through interaction with the viral transcriptional factor Tax as well as CREB. So this mode of the action is quite parallel to the situation with EBV. Because both human T-cell leukemia virus type 1 and EBV are lymphotropic viruses, there is a possibility that other lymphotropic viruses such as the human immunodeficiency virus might also be controlled by TORC proteins.

Curiously, although CMV immediate-early promoter has a CREB binding motif (26), we here observe that transcription from the promoter is less affected by TORC proteins (Fig. 1*C*) when compared with the BZLF1 promoter, an EBV immediate-early gene. Others also have used expression vectors driven by the CMV immediate-early promoter and shown that the promoter activity is relatively unaffected (22, 42). It is speculated that this might be because the activation by TORC is dependent on the promoter context (11, 43). Because immediate-early genes of herpesviruses are crucial for lytic infection, distinct dependence of the promoters on TORC proteins may reflect differences in the characters of those herpesviruses.

Although TORC proteins could enhance Zp 100-fold in reporter assays, overexpression or ablation of TORC2 had only a relatively small impact on BZLF1 production under physiological conditions. It is likely that transcriptional suppressors of the promoter such as YY1 (44) might inhibit transcription. Another intriguing possibility is that there might be epigenetic regulation such as DNA methylation or histone deacetylation. Interestingly, Gruffat *et al.* (45) reported that myocyte enhancer factor 2 family protein, a crucial transactivator for the

Zp, recruits class II histone deacetylases to suppress transcription from Zp. They argued that the switch from latency to the productive cycle is dependent at least in part on the post-translational modification of myocyte enhancer factor 2 and local acetylation state of histones around the Zp. Likewise, the transcriptional co-activator TORC can associate with BCL-3, which recruits histone deacetylases to inhibit transcription (22). These results and the cited reports suggest that the molecular mechanism regulating EBV reactivation from latency is not quite as simple as expected, and further clarification of the mechanism of BZLF1-mediated transcription is necessary. Elucidation of associating factors and chromosomal environment of the Zp proximity may contribute to the development of anti-EBV compounds.

Acknowledgments—We thank Drs. W. Hammerschmidt and K. Takada for providing the EBV-Bac and Akata cells, respectively. We also express our appreciation to Y. Nishikawa for technical assistance.

REFERENCES

1. Speck, S. H., Chatila, T., and Flemington, E. (1997) *Trends Microbiol.* **5,** 399–405
2. Amon, W., and Farrell, P. J. (2005) *Rev. Med. Virol.* **15,** 149–156
3. Tsurumi, T., Fujita, M., and Kudoh, A. (2005) *Rev. Med. Virol.* **15,** 3–15
4. Flemington, E., and Speck, S. H. (1990) *J. Virol.* **64,** 1217–1226
5. Liu, S., Liu, P., Borras, A., Chatila, T., and Speck, S. H. (1997) *EMBO J.* **16,** 143–153
6. Liu, S., Borras, A. M., Liu, P., Suske, G., and Speck, S. H. (1997) *Virology* **228,** 11–18
7. Liu, P., Liu, S., and Speck, S. H. (1998) *J. Virol.* **72,** 8230–8239
8. Ruf, I. K., and Rawlins, D. R. (1995) *J. Virol.* **69,** 7648–7657
9. Flemington, E., and Speck, S. H. (1990) *J. Virol.* **64,** 1227–1232
10. Iourgenko, V., Zhang, W., Mickanin, C., Daly, I., Jiang, C., Hexham, J. M., Orth, A. P., Miraglia, L., Meltzer, J., Garza, D., Chirn, G. W., McWhinnie, E., Cohen, D., Skelton, J., Terry, R., Yu, Y., Bodian, D., Buxton, F. P., Zhu, J., Song, C., and Labow, M. A. (2003) *Proc. Natl. Acad. Sci. U. S. A.* **100,** 12147–12152
11. Conkright, M. D., Canettieri, G., Screaton, R., Guzman, E., Miraglia, L., Hogenesch, J. B., and Montminy, M. (2003) *Mol. Cell* **12,** 413–423
12. Screaton, R. A., Conkright, M. D., Katoh, Y., Best, J. L., Canettieri, G., Jeffries, S., Guzman, E., Niessen, S., Yates, J. R., III, Takemori, H., Okamoto, M., and Montminy, M. (2004) *Cell* **119,** 61–74
13. Bittinger, M. A., McWhinnie, E., Meltzer, J., Iourgenko, V., Latario, B., Liu, X., Chen, C. H., Song, C., Garza, D., and Labow, M. (2004) *Curr. Biol.* **14,** 2156–2161
14. Goldfeld, A. E., Liu, P., Liu, S., Flemington, E. K., Strominger, J. L., and Speck, S. H. (1995) *Virology* **209,** 225–229
15. Delecluse, H. J., Hilsendegen, T., Pich, D., Zeidler, R., and Hammerschmidt, W. (1998) *Proc. Natl. Acad. Sci. U. S. A.* **95,** 8245–8250
16. Tatsumi, Y., Sugimoto, N., Yugawa, T., Narisawa-Saito, M., Kiyono, T., and Fujita, M. (2006) *J. Cell Sci.* **119,** 3128–3140
17. Kanamori, M., Tajima, M., Satoh, Y., Hoshikawa, Y., Miyazawa, Y., Okinaga, K., Kurata, T., and Sairenji, T. (2000) *Virus Genes* **20,** 117–125
18. Kudoh, A., Fujita, M., Kiyono, T., Kuzushima, K., Sugaya, Y., Izuta, S., Nishiyama, Y., and Tsurumi, T. (2003) *J. Virol.* **77,** 851–861
19. Takada, K., Horinouchi, K., Ono, Y., Aya, T., Osato, T., Takahashi, M., and Hayasaka, S. (1991) *Virus Genes* **5,** 147–156
20. Daikoku, T., Kudoh, A., Sugaya, Y., Iwahori, S., Shirata, N., Isomura, H., and Tsurumi, T. (2006) *J. Biol. Chem.* **281,** 11422–11430
21. Koga, H., Ohshima, T., and Shimotohno, K. (2004) *J. Biol. Chem.* **279,** 52978–52983
22. Hishiki, T., Ohshima, T., Ego, T., and Shimotohno, K. (2007) *J. Biol. Chem.* **282,** 28335–28343
23. Ego, T., Tanaka, Y., and Shimotohno, K. (2005) *Oncogene* **24,** 1914–1923
24. Murata, T., and Shimotohno, K. (2006) *J. Biol. Chem.* **281,** 20788–20800
25. Daikoku, T., Kudoh, A., Fujita, M., Sugaya, Y., Isomura, H., and Tsurumi, T. (2004) *J. Biol. Chem.* **279,** 54817–54825
26. Lang, D., Fickenscher, H., and Stamminger, T. (1992) *Nucleic Acids Res.* **20,** 3287–3295
27. Taylor, N., Flemington, E., Kolman, J. L., Baumann, R. P., Speck, S. H., and Miller, G. (1991) *J. Virol.* **65,** 4033–4041
28. Koo, S. H., Flechner, L., Qi, L., Zhang, X., Screaton, R. A., Jeffries, S., Hedrick, S., Xu, W., Boussouar, F., Brindle, P., Takemori, H., and Montminy, M. (2005) *Nature* **437,** 1109–1111
29. Kuraishy, A. I., French, S. W., Sherman, M., Herling, M., Jones, D., Wall, R., and Teitell, M. A. (2007) *Proc. Natl. Acad. Sci. U. S. A.* **104,** 10175–10180
30. Dentin, R., Liu, Y., Koo, S. H., Hedrick, S., Vargas, T., Heredia, J., Yates, J., III, and Montminy, M. (2007) *Nature* **449,** 366–369
31. Ravnskjaer, K., Kester, H., Liu, Y., Zhang, X., Lee, D., Yates, J. R., III, and Montminy, M. (2007) *EMBO J.* **26,** 2880–2889
32. Daikoku, T., Kudoh, A., Fujita, M., Sugaya, Y., Isomura, H., Shirata, N., and Tsurumi, T. (2005) *J. Virol.* **79,** 3409–3418
33. Arimoto, K., Takahashi, H., Hishiki, T., Konishi, H., Fujita, T., and Shimotohno, K. (2007) *Proc. Natl. Acad. Sci. U. S. A.* **104,** 7500–7505
34. Bryant, H., and Farrell, P. J. (2002) *J. Virol.* **76,** 10290–10298
35. Zhang, Q., Gutsch, D., and Kenney, S. (1994) *Mol. Cell. Biol.* **14,** 1929–1938
36. Kudoh, A., Fujita, M., Zhang, L., Shirata, N., Daikoku, T., Sugaya, Y., Isomura, H., Nishiyama, Y., and Tsurumi, T. (2005) *J. Biol. Chem.* **280,** 8156–8163
37. Wu, F. Y., Chen, H., Wang, S. E., ApRhys, C. M., Liao, G., Fujimuro, M., Farrell, C. J., Huang, J., Hayward, S. D., and Hayward, G. S. (2003) *J. Virol.* **77,** 1481–1500
38. Morrison, T. E., and Kenney, S. C. (2004) *Virology* **328,** 219–232
39. Deng, Z., Chen, C. J., Zerby, D., Delecluse, H. J., and Lieberman, P. M. (2001) *J. Virol.* **75,** 10334–10347
40. Adamson, A. L., and Kenney, S. (1999) *J. Virol.* **73,** 6551–6558
41. Zerby, D., Chen, C. J., Poon, E., Lee, D., Shiekhattar, R., and Lieberman, P. M. (1999) *Mol. Cell. Biol.* **19,** 1617–1626
42. Siu, Y. T., Chin, K. T., Siu, K. L., Yee Wai Choy, E., Jeang, K. T., and Jin, D. Y. (2006) *J. Virol.* **80,** 7052–7059
43. Xu, W., Kasper, L. H., Lerach, S., Jeevan, T., and Brindle, P. K. (2007) *EMBO J.* **26,** 2890–2903
44. Montalvo, E. A., Cottam, M., Hill, S., and Wang, Y. J. (1995) *J. Virol.* **69,** 4158–4165
45. Gruffat, H., Manet, E., and Sergeant, A. (2002) *EMBO Rep.* **3,** 141–146

JOURNAL OF VIROLOGY, July 2009, p. 6922–6928 Vol. 83, No. 13
0022-538X/09/$08.00+0 doi:10.1128/JVI.02674-08

Genetic Analysis of Hepatitis C Virus with Defective Genome and Its Infectivity in Vitro▽

Kazuo Sugiyama,[1]* Kenji Suzuki,[2] Takahide Nakazawa,[3] Kenji Funami,[1] Takayuki Hishiki,[4] Kazuya Ogawa,[4] Satoru Saito,[5] Kumiko W. Shimotohno,[2] Takeshi Suzuki,[2] Yuko Shimizu,[1] Reiri Tobita,[6] Makoto Hijikata,[7] Hiroshi Takaku,[6] and Kunitada Shimotohno[1,4]

Center for Integrated Medical Research, Keio University, Shinjuku-ku, Shinanomachi 35, Tokyo 160-8582, Japan[1]; Division of Basic Biological Sciences, Faculty of Pharmacy, Keio University, Tokyo 105-8512, Japan[2]; Department of Gastroenterology, Internal Medicine, Kitasato University East Hospital, Kanagawa 228-8520, Japan[3]; Research Institute, Chiba Institute of Technology, Chiba 275-0016, Japan[4]; Yokohama City University Hospital, Kanagawa 236-0004, Japan[5]; Department of Life and Environmental Sciences, Chiba Institute of Technology, Chiba 275-0016, Japan[6]; and Institute for Virus Research, Kyoto University, Kyoto 606-8507, Japan[7]

Received 29 December 2008/Accepted 6 April 2009

Replication and infectivity of hepatitis C virus (HCV) with a defective genome is ambiguous. We molecularly cloned 38 HCV isolates with defective genomes from 18 patient sera. The structural regions were widely deleted, with the 5′ untranslated, core, and NS3-NS5B regions preserved. All of the deletions were in frame, indicating that they are translatable to the authentic terminus. Phylogenetic analyses showed self-replication of the defective genomes independent of full genomes. We generated a defective genome of chimeric HCV to mimic the defective isolate in the serum. By using this, we demonstrated for the first time that the defective genome, as it is circulating in the blood, can be encapsidated as an infectious particle by *trans* complementation of the structural proteins.

Viruses with a deletion mutation in their genome have been identified as defective interfering (DI) particles for many virus species (1, 3, 9, 16). Part of the DI virus genome is deleted, but regions indispensable for replication and packaging are preserved. Most DI viruses occur spontaneously in the course of cell culture infected with a high titer of wild-type viruses. Hepatitis C virus (HCV) with a defective genome has been found in liver and serum specimens of some HCV patients (4, 8, 15). HCV has a plus-strand RNA genome that encodes the viral core, E1, E2, and p7 structural proteins and NS2, NS3, NS4A, NS4B, NS5A, and NS5B nonstructural proteins (10). According to the reports, the deletions have been found mainly in the structural region and most of the deletions are in frame, but some deletions are out of frame (4), raising questions about whether the defective HCV genome is merely a by-product of a full genome or a self-replicating genome and whether it can be encapsidated into an infectious virus particle.

In the present study, we molecularly cloned 38 HCV isolates with defective genomes from HCV patient sera to address these questions by genetic analyses and infection experiments. As long as we explored, all of the deletions were in frame, indicating the potential to support translation from the authentic initiation codon to the termination codon, although the structural region was widely deleted, as reported previously. Phylogenetic analyses evidenced self-replication of the defective genomes independent of full genomes. We demonstrated for the first time, by *trans* complementation experiments, that the defective genome, as it is circulating in the blood, can be encapsidated as an infectious particle, designated HCV_{CCD}.

First, to amplify HCV cDNAs in 21 serum specimens from 18 HCV patients (genotype 1b), we performed three sets of long-distance reverse transcription (RT)-PCRs flanking (i) the 5′ untranslated region (UTR) to the 5′ part of the NS3 region, (ii) the remaining part of the NS3 region to the end of NS5B, and (iii) the 5′ UTR to the end of the NS5B region (Fig. 1A). The specimens were collected with informed consent. cDNA was synthesized with RNase H-deficient reverse transcriptase Superscript III (Invitrogen, Carlsbad, CA) at a higher temperature (55°C) to reduce template switching and mispriming. PCRs were performed in a (hemi)nested manner with high-fidelity polymerase KOD plus or KOD FX (Toyobo, Osaka, Japan) as described previously (5). For some target nucleotide positions, a mixture of two or three primers was used to reduce mismatches due to sequence heterogeneity (Table 1). Of the 21 specimens examined, representative results are shown in Fig. 1. An amplicon of the 5′ UTR-NS3 region of the predicted size (ca. 3.7 kb) was detected in all specimens (18/18), and representative results are shown in Fig. 1B. In addition, a shorter amplicon suggestive of a defective HCV genome was simultaneously present in four specimens from 1 (R4) of 12 cases of clinically mild hepatitis and from 3 (T5, K3, and K4-pre) of 6 cases of active hepatitis (clinical data not shown). Defective genomes were found in the patients with relatively higher copy numbers of HCV RNA ($>8.1 \times 10^5$ copies/ml in the 5′ UTR, Table 2), suggesting that the coexistence of a defective genome is related to hepatitis severity. The authentic-size amplicon was poorly detected when coexisting with a defective HCV genome shorter than 2 kb (T5 and K3), presumably because of preferential amplification of the shorter amplicon. A shorter amplicon was not detected for the NS3-

* Corresponding author. Mailing address: Center for Integrated Medical Research, Keio University, Shinjuku-ku, Shinanomachi 35, Tokyo 160-8582, Japan. Phone: 81-3-3353-1211. Fax: 81-47-478-0527. E-mail: sygiyamkz@a8.keio.jp.

▽ Published ahead of print on 15 April 2009.